

## **Abstract**

Title: **EXPERIMENTAL AND COMPUTATIONAL ANALYSIS OF THE FIRE SUPPRESSION EFFECTIVENESS OF HALON 1301 REPLACEMENTS**

**John L. Pagliaro, Master of Science, 2012**

Directed By: **Associate Professor Peter B. Sunderland,  
Department of Fire Protection Engineering**

Experimental and computational work was performed to help understand why sub-inerting concentrations of HFC-125 ( $C_2HF_5$ ) produced overpressures in the FAA aerosol can explosion test. The fire suppression performance of HCFC-123 ( $C_2HCl_2F_3$ ) was also investigated to determine whether it may perform better than HFC-125. Thermodynamic analysis shows that both agents increase the overall heat release for lean mixtures containing the aerosol can contents. HFC-125 also increases the overall reaction rate when added to lean mixtures. The overall reaction rate of mixtures containing HCFC-123 is generally lowered when sub-inerting concentrations are added. Experimental results showed that HCFC-123 has a lower minimum inerting concentration (8.9%) than HFC-125 (13.5%). Mixtures containing HCFC-123 were found to produce peak pressures in the 2 L chamber that were estimated to cause overpressures in the FAA chamber. Nitrogen dilution resulting in 20% oxygen in air was successful at eliminating the overpressure of mixtures containing HCFC-123.

EXPERIMENTAL AND COMPUTATIONAL ANALYSIS OF THE FIRE SUPPRESSION  
EFFECTIVENESS OF HALON 1301 REPLACEMENTS

By  
John L. Pagliaro

Thesis submitted to the Faculty of the Graduate School of the  
University of Maryland, College Park, in partial fulfillment  
of the requirements for the degree of  
Master of Science  
2012

Advisory Committee:  
Associate Professor Peter B. Sunderland, chair  
Dr. Gregory T. Linteris, NIST Senior Research Scientist  
Assistant Professor Stanislav I. Stoliarov

© Copyright by

John L. Pagliaro

2013

## **Acknowledgements**

I would like begin by expressing my gratitude to Dr. Peter Sunderland for being my academic advisor. Thanks for being ambitious and recognizing the opportunity for us to assist in the project at NIST. I am very much appreciative of the opportunity that I have been given to pursue a master's degree in a field that I enjoy. Dr. Sunderland has provided superb guidance during the entire journey and has given helpful suggestions and references pertaining to the work at hand. Dr. Sunderland truly cares for the wellbeing of his students and I would like to thank him for that.

While at NIST I have had the opportunity to work with research scientists that are leading experts in their fields. Dr. Gregory Linteris is the lead researcher on the project that I am a part of. Working with Dr. Linteris was, and will continue to be, one of the most influential experiences of my life. He is truly passionate about the work he does and about the contributions he makes. His work ethic alone is motivating as it shows what you can achieve when you give it your all. Dr. Linteris has extended his knowledge of combustion fundamentals and laboratory etiquette and for that I would like to thank him.

I would like to thank the NIST-ARRA fellowship program at the University of Maryland for providing the funding for my work. I would also like to thank The Boeing Company and Honeywell for contributing funding toward projects that I worked on. Thanks to the machinists at NIST how helped construct the experimental apparatus, specifically Ed Hnetkovsky and Marco Hernandez. Thanks to Dr. Babushok, for whom I share an office with, for sharing his knowledge of combustion chemistry.

The fire protection engineering faculty and staff deserve thanks as they work hard every day to continue to grow the reputation of the department. My research has been enjoyable yet challenging at times and I feel so fortunate for the opportunity that I have been given to work with people of such caliber. I hope the next few years are just as rewarding as I continue my studies.

# Table of Contents

Acknowledgements.....	ii
List of Tables .....	vi
List of Figures .....	vii
List of Abbreviations .....	ix
1. Introduction.....	1
1.1 Montreal Protocol .....	1
1.2 Halon 1301 Replacement in Aircraft Cargo Bay Fire Suppression Systems.....	1
1.3 Federal Aviation Administration Aerosol Can Explosion Test .....	2
1.4 Goals and Objectives .....	4
1.5 Justification for Studying HCFC-123 .....	5
2. Approach.....	8
2.1 2L Chamber Setup .....	8
2.2 Measurement Devices .....	10
2.3 Ignition Method .....	10
2.4 Operating Procedure .....	13
2.5 Assumptions to Simplify ACT Analysis.....	14
2.6 Description of Premixed Zone .....	15
2.7 Converting FAA Chamber Mixtures to 2L Chamber Mixtures.....	16
2.8 Determination of Aerosol Can Fuel Equivalent (ACTe) .....	18
2.9 Relating Chamber Volume Fraction to Equivalence Ratio.....	20
3. Computational Analysis.....	22
3.1 Thermodynamic Equilibrium Calculations.....	22
3.2 Perfectly Stirred Reactor Calculations.....	27
4. Experimental Results .....	36
4.1 Determination of Experimental Mixtures .....	36
4.2 Relating 2L Chamber Pressure Rise to FAA Chamber Pressure Rise.....	39
4.3 Test Results for HFC-125 .....	40
4.3.1 Effects of Water Vapor on Peak Pressure Rise.....	41

4.3.2 Effect of Nitrogen Dilution on Peak Pressure Rise .....	44
4.4 Test Results for HCFC-123 .....	46
4.4.1 Effects of Water Vapor .....	47
4.4.2 Effects of Nitrogen Dilution .....	48
4.5 HCFC-123 vs. HFC-125 .....	48
5. Conclusions .....	50
5.1 Future Work .....	52
Appendices .....	53
1. 2L Chamber Schematics .....	53
2. Pressure Vessel Safety Considerations .....	55
3. LabView VI Block Diagram and Front Panel.....	57
4. Complete List of Procedures.....	59
5. Summary of FAA Test Results with Mixture Conversion to 2L Chamber .....	64
6. CEA2 Equilibrium Script.....	67
References .....	69

## List of Tables

Table 1: Summary of the FAA aerosol can test results. ....	4
Table 2: Environmental impact of HCFCs currently in use. ....	5
Table 3: Environmental impact of Halon 1301 and its potential replacements.....	6
Table 4: Peak pressure rise comparison of mixtures containing actual aerosol can fuel and ACTe fuel. ....	20
Table 5: Summary of tests conducted with a chamber volume fraction ( $\eta$ ) of 0.5 ( $\Phi=0.57$ ) with various relative humidity and oxygen concentrations. ....	39
Table 6: Comparison of FAA chamber pressure rise to the predicted pressure rise based on peak pressure measured in 2L chamber.....	41



## List of Figures

Figure 1: Illustration of the constant volume chamber used during the FAA aerosol can tests [7].	3
Figure 2: 2 L constant volume combustion chamber used to collect experimental data. ....	9
Figure 3: 2L chamber igniter feedthrough with a platinum wire crimed connected. ....	12
Figure 4: Illustration of simplified flame types present during aerosol can tests [20]. ....	15
Figure 5: 2L mixture relative humidity based on the chamber volume fraction ( $\eta$ ) assumed to mix with the aerosol can contents in the FAA chamber. ....	17
Figure 6: Mixture equivalence ratio ( $\Phi$ ) based on the chamber volume fraction ( $\eta$ ) assumed to mix with ACTe fuel. The upper and lower flammability limits of the propane fuel component are also presented as bounds for which flammable mixtures are expected. ....	21
Figure 7: Constant volume peak pressure for Halon 1301/air/ACTe mixtures as a function of percent Halon 1301 added in air for various mixture equivalence ratios ( $\Phi$ ). ....	24
Figure 8: Constant volume peak pressure for HFC-125/air/ACTe mixtures as a function of percent HFC-125 added in air for various mixture equivalence ratios ( $\Phi$ ). ....	25
Figure 9: Constant volume peak pressure for HCFC-123/air/ACTe mixtures as a function of percent HCFC-123 added in air for various mixture equivalence ratios ( $\Phi$ ). ....	26
Figure 10: Comparison of the peak pressure rise of mixtures containing HFC-125 (solid lines) and HCFC-123 (dashed lines) for an equivalence ratio ( $\Phi$ ) of 0.7, 0.5, and 0.4. ....	27
Figure 11: Overall reaction rate ( $\omega_{psr}$ ) for Halon 1301/air/ACTe mixtures as a function of percent Halon 1301 added in air for various mixture equivalence ratios ( $\Phi$ ). ....	30
Figure 12: Overall reaction rate ( $\omega_{psr}$ ) for HFC-125/air/ACTe mixtures as a function of percent HFC-125 added in air for various mixture equivalence ratios ( $\Phi$ ). ....	32

Figure 13: Overall reaction rate ( $\omega_{psr}$ ) for HCFC-123/air/ACTe mixtures as a function of percent HCFC-123 added in air for various mixture equivalence ratios ( $\Phi$ ). ..... 33

Figure 14: Comparison of the overall reaction rate ( $\omega_{psr}$ ) of mixtures containing HFC-125 (solid lines) and HCFC-123 (dashed lines) for an equivalence ratio ( $\Phi$ ) of 0.7, 0.5, and 0.4. .... 34

Figure 15: Chamber volume fraction (pink) that produces the peak adiabatic flame temperature (blue) for mixtures containing the actual aerosol can contents and HFC-125. .... 38

Figure 16: Peak pressure rise in 2 L chamber for mixtures containing ACTe fuel, air, and HFC-125 with a relative humidity of 100% (solid line) and a relative humidity of 0% (dotted line). The chamber volume fraction involved ( $\eta$ ) is 0.5. .... 42

Figure 17: Equilibrium adiabatic flame temperature for mixtures containing ACTe fuel, air, and HFC-125 with a relative humidity of 100% (solid line) and a relative humidity of 0% (dotted line). The chamber volume fraction involved ( $\eta$ ) is 0.5. .... 43

Figure 18: Perfectly stirred reactor prediction of the overall reaction rate for mixtures containing ACTe fuel, air, and HFC-125 with a relative humidity of 100% (solid line) and a relative humidity of 0% (dotted line). The chamber volume fraction involved ( $\eta$ ) is 0.5. .... 44

Figure 19: Peak pressure rise of HFC-125 mixtures containing 21%, 20%, and 19% oxygen in air. The chamber volume fraction involved ( $\eta$ ) is 0.5. The horizontal dotted line represents the maximum allowable peak pressure in the 2L chamber that will not create an overpressure in the FAA chamber. .... 46

Figure 21: Peak pressure rise comparison of mixtures containing HFC-125 (blue) and HCFC-123 (red). .... 49

## **List of Abbreviations**

ODS – Ozone depleting substance

CFCs - Chlorofluorocarbons

HCFCs - Hydrochlorofluorocarbons

Halons - Halogenated hydrocarbons

HFCs - Hydrofluorocarbons

FAA – Federal Aviation Administration

EPA – Environmental Protection Agency

ODP – Ozone depletion potential

GWP – Global warming potential

ACT – Aerosol can test

ACTe – Aerosol can test equivalent mixture

CEA2 – NASA Chemical Equilibrium with Applications (Version 2)

NIST – National Institute of Standards and Technology

PSR – Perfectly stirred reactor simulator

# **1. Introduction**

## **1.1 Montreal Protocol**

In 1987, the Montreal Protocol formally recognized the significant threat of ozone depleting substances (ODSs) to the ozone layer and provided a mechanism to phase out the global production and consumption of ODSs. Regulation No. 2037/2000, established by the protocol, set specific rules on the usage and phase out dates of ODSs including chlorofluorocarbons (CFCs), hydrochlorofluorocarbons (HCFCs), and halogenated hydrocarbons (Halon) [1]. CFCs and HCFCs are chemical substances used primarily as working fluids in refrigeration systems while some applications for HCFCs include usage as a component of fire suppressants, for both streaming and total-flooding uses [2]. They also function as propellants in aerosol and foams, and have some specialized medical uses [3]. Halons have been extensively used as fire suppressants in fire extinguishers and flooding systems. Halons exhibit several favorable fire suppressant characteristics. These substances are non-conductive, which makes them ideal for use with electrical equipment; they do not leave a residue which minimizes damage to equipment; they act very quickly in suppressing fires; and they can be used in occupied spaces as their toxicity is low [4]. The primary replacements for the compounds banned by the Montreal Protocol have been hydrofluorocarbons (HFCs) which have very low ozone depletion potential (ODP) as they do not contain chlorine or bromine.

## **1.2 Halon 1301 Replacement in Aircraft Cargo Bay Fire Suppression Systems**

Currently, a suitable replacement for Halon 1301 ( $\text{CF}_3\text{Br}$ , bromotrifluoromethane) in aircraft applications has not been found. This has led to a critical-use exemption of Halon 1301 by the Montreal Protocol for its fire suppression application in aircraft for the protection of crew compartments, engine nacelles, cargo bays, dry bays, and fuel tank inerting [4]. Although this

exemption was granted, the European Union requires replacement of halon in new design aircraft by 2018, and in existing aircraft by 2040 [5].

The Federal Aviation Administration (FAA) has begun the search for potential halon replacements that exhibit similar suppression effectiveness with lower ozone depletion potential (ODP) and global warming potential (GWP). In 1999, the FAA's Minimum Performance Standard for Aircraft Cargo Compartment Halon Replacement Fire Suppression Systems defined four fire scenarios for which potential replacements would be tested to address the wide variety of fires possible in the cargo compartment of an aircraft. Bulk load, containerized, surface burning, and aerosol can explosion fire scenarios were specified to ensure halon replacements could effectively protect an aircraft cargo bay [6].

### **1.3 Federal Aviation Administration Aerosol Can Explosion Test**

Reinhardt [7] performed aerosol can explosion tests with Halon 1301, HFC-125 ( $C_2HF_5$ , pentafluoroethane), and 2-BTP ( $C_3H_2F_3Br$ , bromotrifluoropropene) in an 11,400 liter constant volume pressure vessel modeled after an aircraft cargo bay. The aerosol can explosion test involves a fire load of 2.05 moles of propane, 5.87 moles of denatured alcohol, and 5.00 moles of liquid water contained in an aerosol can simulator. The test simulates a situation where a fire in an aircraft cargo bay heats up an aerosol can until it explodes, exposing its contents to the fire. The test was designed to ensure that suppressing agents could handle the explosion of a can of hairspray, for instance, that might be located within luggage stored in the cargo bay. In the tests, the aerosol can contents were housed at around 16 bar before a fast-acting valve was switched and the contents were released into the chamber. Ignition was caused by a continuous DC arc across electrodes located 91.4 cm downstream of the valve. The aerosol can contents spread throughout the chamber and mix with the ambient air that contains premixed fire suppressant.

Pressure transducers measure pressure, thermocouples measure temperature, a video camera captures visual images, and gas sampling probes measure the concentration of oxygen and agent during each test. Figure 1 shows a schematic of the setup used during the aerosol can tests [7].

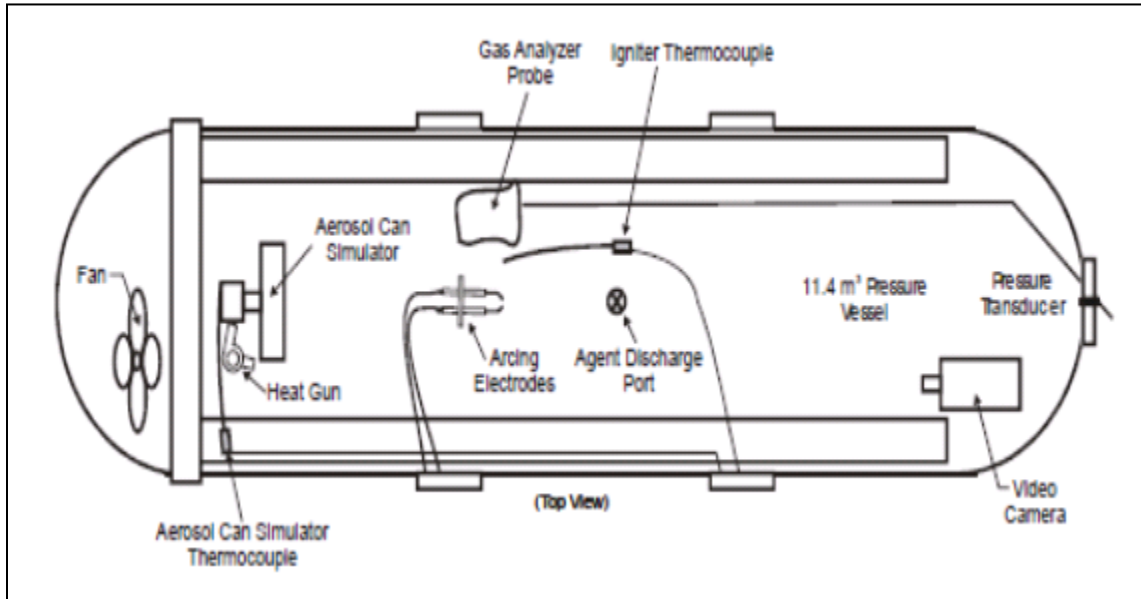


**Figure 1: Illustration of the constant volume chamber used during the FAA aerosol can tests [7].**

The results of the aerosol can explosion test are shown in Table 1. Tests performed without added agent produced an average peak temperature of 180 °C and an average peak pressure rise of 1.7 bar. When Halon 1301 was added to the chamber air at a volume fraction of 2.5%, the peak pressure rise was 0.28 bar. When HFC-125 was added at volume fractions of 6.2%, 8.9%, and 11% the peak pressure rise was found to be about 3.6 bar while when added at 13.5%, no pressure rise occurred. When 2-BTP was added at a volume fraction of 3% and 4% the peak pressure rise was about 4.3 bar, while for 5% and 6% the peak pressure rise was about 6.7 bar. The results of Reinhardt et al show that while there exists a given inerting concentration for both HFC-125 and 2-BTP in the aerosol can explosion test, when added at concentrations

below the inerting concentration, these substances actually increase the peak pressure rise as well as the heat release when compared to the case with no added agent.

**Table 1: Summary of the FAA aerosol can test results.**

Test Number	Agent	Agent Volume Fraction (%)	Initial Temperature (°C)	Fire Event	Peak Temperature (°C)	Peak Pressure Rise (bar)
3	None	0	18.3	Yes	197	1.75
4	None	0	20.0	Yes	164	1.61
16	Halon 1301	2.5	11.8	Yes	18	0.28
5	BTP	3	21.1	Yes	569	4.34
6	BTP	4	18.3	Yes	591	4.34
9	BTP	5	18.9	Yes	677	6.89
13	BTP	6	17.2	Yes	797	6.41
23	HFC-125	6.2	10.0	Yes	552	3.59
17	HFC-125	8.9	N/A	Yes	664	3.65
19	HFC-125	11	N/A	Yes	575	3.59
20	HFC-125	13.5	9.8	No	N/A	N/A

#### 1.4 Goals and Objectives

The goal of the present work is to help understand why sub-inerting concentrations of HFC-125 produce overpressures in the aerosol can test and to investigate potential replacements that were not considered during the original FAA aerosol can tests. HFC-125 clearly failed the aerosol can test when used as the sole suppressing mechanism. Similar cargo bay tests were performed with a water mist system which was also found to be insufficient [8]. The water mist system was then considered in conjunction with a nitrogen system used to reduce the quantity of oxygen present in the chamber. The same concept has been proposed to combine an HFC-125 system with a nitrogen system. The quantity of nitrogen required for the HFC-125 system to pass the aerosol can test has been examined.

While studying the effectiveness of HFC-125 as a flooding agent, HCFC-123 (dichlorotrifluoroethane,  $C_2HCl_2F_3$ ) was also investigated to determine whether it may potentially perform better than HFC-125 in the FAA aerosol can test. HCFC-123 and HFC-125 are chemically similar with the only difference being the substitution of two fluorine atoms with chlorine atoms. Babashok et al numerically predicted that HCFC compounds are more effective flame inhibitors than similar HFC compounds with substituted chlorine atoms [36].

### 1.5 Justification for Studying HCFC-123

It is important to note that as the treaty stands, HCFC-123 will eventually be banned by the Montreal Protocol, as previously mentioned. Although the original provisions of the Montreal Protocol did not place any bans on HCFCs, several amendments have led to an agreement to halt HCFC production in developed countries by 2030 [9]. Table 2 provides a comparison of the atmospheric lifetime ( $t_{atm}$ ), GWP, and ODP of various HCFCs currently in use [10, 11]. HCFC-123 has the lowest value in all three categories.

**Table 2: Environmental impact of HCFCs currently in use.**

HCFC Compound	Chemical Formula	$t_{atm}$ (yr)	ODP	GWP
22	$CHClF_2$	12	0.05	1810
123	$C_2HCl_2F_3$	1.3	0.02	77
124	$CHClFCF_3$	5.8	0.022	609
142b	$CH_3CClF_2$	17.9	0.07	2310

Next, it is of interest to compare the environmental impacts of HCFC-123 to that of HFC-125 and Halon 1301. Table 3 shows that although HCFC-123 has a much higher ODP than the practically zero value for HFC-125, it has the shortest atmospheric lifetime and lowest GWP [10,



11]. The ODP is also orders of magnitude less than Halon 1301 which would make it a more environmentally friendly replacement if it can pass the FAA aerosol can test.

**Table 3: Environmental impact of Halon 1301 and its potential replacements.**

Suppression Compound	Chemical Formula	$t_{\text{atm}}$ (yr)	ODP	GWP
Halon 1301	$\text{CF}_3\text{Br}$	65	12	5400
HFC-125	$\text{C}_2\text{HF}_5$	29	0.00003	3500
HCFC-123	$\text{C}_2\text{HCl}_2\text{F}_3$	1.3	0.02	77

Although HCFC-123 is scheduled to be banned by 2030, studies have been performed [2, 12] with the aim of quantifying ozone depletion resulting from the release of HCFC-123 and potential depletion of continued use of HCFC-123 if an exception were to be made by the Montreal Protocol. Wuebbles et al [12] claim that “analysis of the projected uses and emissions of HCFC-123, assuming reasonable levels of projected growth and use in centrifugal chiller and fire suppressant applications, suggests an extremely small impact on the environment due to its short atmospheric lifetime, low ODP, low GWP, and the small production and emission of its limited applications. The current contribution of HCFC-123 to stratospheric reactive chlorine is too small to be measured.”

When Wuebbles et al [12] performed the study, the use of HCFC-123 was only considered in fire suppression applications involving streaming systems. These systems use Halotron I as the main suppressing agent which is comprised of 95% HCFC-123 by weight. The additional amount of HCFC-123 that would be needed for cargo bay suppression systems was not taken into consideration although the amount that may be released into the environment if used as a cargo bay suppressant can be estimated based on the number of reported cargo bay fires that have occurred in the past. This is similar to the technique of estimating the leakage rate

of HCFC-123 when used in centrifugal chillers as the total amount of refrigerant present in all chillers is not the amount considered to be released into the atmosphere. The FAA records show an average of 4 cargo bay fires per year between 1976 and 1996 [13]. The increase in the amount of HCFC-123 into the atmosphere would be minimal if it was assumed that HCFC-123 is released only during a cargo bay fire event.

Several factors must be considered during the selection process of a Halon 1301 replacement. Although HFC-125 does not deplete the ozone layer, it still has a high GWP. Recent proposals have been made to control HFC use by amending the Montreal Protocol. Critics of the Montreal Protocol, as it stands, argue that the climate benefit may be reduced or lost completely in the future if the emissions of ODS substitutes with high GWPs, such as long-lived HFCs, continues to increase [14, 15]. If HFCs are banned then that further reduces the available compounds that may be considered as replacements. Although research efforts continue in an attempt to find a Halon 1301 replacement, no molecule that possesses all the desired properties of the ideal halon have been found and may never be found [16]. Thus, agent selection will continue to be application-specific, requiring consideration of the performance, safety, and environmental characteristics of the different clean agents [16]. HCFC-123 is not an ideal clean agent but if the performance is found to be comparable to Halon 1301 it may be a viable replacement. After all, Halotron I was approved in 1994 under the EPA's Significant New Alternatives Program as a Halon 1211 replacement agent for streaming systems [12]. Similar exemptions from an environmental standpoint could be made in the future with regard to Halon 1301.

## 2. Approach

### 2.1 2L Chamber Setup

Constant volume combustion experiments were conducted in a 2.54 cm thick, 316 stainless steel spherical chamber with an inner diameter of 15.24 cm. The chamber consists of two hemispherical sections, each machined out of a block of stainless steel to create two flanged sections with no seams or welds. The hemispherical sections were secured together by eight 3/8" diameter bolts. One hemispherical section has an o-ring groove machined into it so that when the sections are bolted together a fluoropolymer o-ring creates a pressure tight seal between them. The chamber design was based off of previous designs [17, 18] which were used to perform similar combustion experiments. Plumbing and electrical schematics are presented in Appendix 1.

Nine tapered ports were machined into the chamber so that various valves, feedthroughs, and measurement devices could be connected. A needle valve was connected to supply gaseous mixtures to the chamber. Upstream from the needle valve was a 5-way valve used to introduce air, fuel, agent, and nitrogen. A needle valve was connected to the chamber as an exhaust path to the laboratory gas handling system. A quarter turn valve with a septum inserted upstream from the valve was connected to allow for liquid injection with a syringe. The liquid injection port was designed to be pressure tight during injection as well as during combustion as the quarter turn valve could be closed. A toggle valve was connected to create a high pressure (11 bar) nitrogen input that was used after each test to cool the product gases before the exhaust valve was opened. The nitrogen input was also used to purge the chamber after opening the exhaust valve. A Swagelok pressure relief valve with a maximum working pressure of 34.5 bar was connected to the chamber as an extra measure of safety. The pressure relief valve was set at 11.7 bar and

tested periodically to ensure any pressure above the predicted operating pressure would trigger the relief valve. The predicted maximum operating pressure was taken from constant volume equilibrium calculations for various hydrocarbon/air mixtures. Other safety precautions, presented in Appendix 2, were taken prior to performing experiments in the 2 L chamber which included pressure vessel stress calculations and hydrostatic testing as recommended by ASTM. The 2 L chamber setup is presented in Figure 2.



**Figure 2: 2 L constant volume combustion chamber used to collect experimental data.**

## **2.2 Measurement Devices**

The chamber was equipped an Omega DP87 digital strain indicator with a pressure range of 0 MPa to 1.33 MPa to allow for partial pressure mixing. The strain indicator was connected through a needle valve so that it could be used at low pressure for mixing and then sealed from the chamber so that combustion pressures would not cause damage. The DP87 gauge has a claimed accuracy of 13.3 kPa which is 1% of the full scale reading and was calibrated against a Baratron 627D absolute pressure transducer. The uncertainty in the pressure measurement was estimated to be 2% of the reading based on this calibration. A PCB Piezotronics dynamic pressure sensor (model 101A06) was employed to measure the dynamic pressure rise resulting from combustion. A type K Omega thermocouple was attached to record temperature. The pressure gauges and thermocouple can be seen in Figure 2 and in the plumbing and electrical schematics presented in Appendix 1. The dynamic pressure sensor and the thermocouple were connected to a National Instruments DAQ and a LabView VI was developed to record and tabulate the measurements. The LabView VI front panel and block diagram can be seen in Appendix 3.

## **2.3 Ignition Method**

The bottom vertical port was designated for ignition and a section of metal sheathed, mineral insulated cable was inserted to create a pressure tight and electrically insulated feedthrough. Central ignition was initiated by fusing a platinum wire 20 mm in length and 0.3 mm in diameter that was connected to the end of the feedthrough. The energy released as the wire fuses was estimated using two different approaches. First, the ignition energy was assumed to be equivalent to the energy required to heat the wire to the melting point plus the latent heat of

fusion. Another variable was introduced which took into account the percentage of wire that was melted before the continuity of the circuit was interrupted. Equation 1 shows this relationship.

$$E_{ign} = mc_p(T_l - T_\infty) + \alpha mh_f \quad (1)$$

Where  $E_{ign}$  is the ignition energy,  $m$  is the mass of platinum,  $c_p$  is the specific heat,  $T_l$  is the melting point,  $T_\infty$  is the ambient temperature,  $\alpha$  is the percentage of wire melted, and  $h_f$  is the heat of fusion. The ignition energy was estimated to be between 7 J and 10 J (both for 0% and 100% of the wire melted).

The second method for predicting the ignition energy was to measure the temperature increase of an inert mixture that results from fusing the platinum wire. The temperature rise and the ideal gas law can be used to determine the energy released based on the heat capacity of the inert gas used during testing. Temperature measurements were recorded during ignition with the chamber filled with air and nitrogen. The two tests yielded ignition energies of 23 J and 9 J respectively. This calculation should be taken as a ballpark estimation as the extent of uniform heating within the chamber is unknown. The two methods of predicting the ignition energy created from a fusing platinum wire produced ignition energy estimations that are the same order of magnitude. The energy required to produce the measured temperature rise in the nitrogen mixture (9 J) was within the estimated energy required to fuse the platinum wire (7-10 J).

Platinum wire ignition was chosen for the following reasons:

1. Simplicity compared to spark ignition system. The platinum wire igniter could be made available much sooner than the spark ignition system and time constraints justified the selection.

2. The overdriven nature of the platinum wire ignition was similar to the overdriven nature of the aerosol can test ignition system. Minimum ignition energies for hydrocarbon/air mixtures are on the order of 1 mJ [19]. Even if added suppressant increases the minimum ignition energy the energy released during the platinum wire ignition was estimated to be orders of magnitude larger than required to ignite hydrocarbon/air mixtures.

The ends of the platinum wire were crimped into connector pins which were then inserted into connector sockets that were crimped to the ends of the igniter. The igniter consisted of two parallel copper electrodes (57 mm long, 1mm diameter) separated by 4 mm. The electrodes were housed in a mineral insulated cable in order to create a pressure tight seal between the chamber and the ambient environment as well as electrical isolation from the chamber. Figure 3 shows the igniter with a platinum wire connected between the electrodes. The other end of the igniter was connected to a standard power cord which was plugged into a variable transformer AC power supply (Powerstat, model 30N116C) set at 100 V.



**Figure 3: 2L chamber igniter feedthrough with a platinum wire crimped connected.**

## 2.4 Operating Procedure

The 2 L chamber was pressure tested and vacuum tested at the beginning of each testing day to ensure the chamber was leak-free. The chamber was then evacuated for five minutes with a vacuum pump. After evacuation, the chamber was purged with dry air for two minutes. The ignitor was installed and the chamber was evacuated below 1 Torr before sample liquids and gases were added to the chamber.

Sample compounds were added to the evacuated chamber using the method of partial pressure mixing. Liquids components were added to the chamber first to reduce the time of vaporization. Liquids were drawn into a syringe and the liquid mass was measured using a Mettler PE 360 DeltaRange. The scale has a reproducibility of 0.003 g and a results deviation of  $\pm 0.003$  g. The sample liquids were then injected into the chamber through a vacuum tight septum. The order in which liquids were injected into the chamber was based on vapor pressure, with the lowest vapor pressure liquids injected first. Sample liquids used during experiments included house de-ionized water, ethanol (The Warner-Graham Company, 200 proof, anhydrous), and HCFC-123. Sample gases were introduced into the chamber after the liquid components were injected. The sample gases used during experiments were propane (Scott Specialty Gases INC., 99.0% purity), nitrogen (GTS-Welco Inc., 99.95% purity), Halon 1301 (Great Lakes Chemical Corp), and HFC-125 (Allied Signal Chemicals, 99.5% purity). The air was house compressed air (filtered and dried) which was additionally cleaned by with a 0.01  $\mu\text{m}$  filter, a carbon filter, and a desiccant bed to remove small aerosols, organic vapors, and water vapor. The relative humidity of the dry shop air was measured with a humidity meter (TSI VELOCICALC model 8386) and found to be between 0% and 2%. Once the final gaseous



mixture component was added to the chamber, five minutes was given to allow the contents to completely mix and settle as suggested by Metgelchi et al [17].

Once partial pressure mixing was completed the Powerstat power source was manually switched on, delivering 100V, before being switched off. As the power source is switched on, the platinum wire fuses due to high current, thereby generating a thermal ignition source. The igniter feedthrough was disconnected and measurement data collected during combustion was stored in an excel file.

The chamber was exhausted and purged with nitrogen after each experiment. Nitrogen was supplied at 11 bar for five seconds before the exhaust valve was opened. This reduces the temperature of the hot product gases before they passed through the exhaust valve. Once the exhaust valve was opened the nitrogen purge lasted for one minute. After the nitrogen purge, the chamber was evacuated for five minutes using a vacuum pump. Dry air was used to purge the chamber for two minutes in order to ensure the product gases were completely flushed. This process of evacuating the chamber then flushing the chamber with dry air was repeated 3 more times. A complete list of procedures used while performing experiments is presented in Appendix 4.

## **2.5 Assumptions to Simplify ACT Analysis**

The fire resulting from the aerosol can explosion is complex making it difficult to examine from first principles. The approach taken was to break down the entire reaction into sections which resemble simpler flame types and to examine these sections using computational and experimental tools. Figure 4, created by Linteris et al [20] illustrates the various regions within the test chamber that resemble simplified flame structures. The partially premixed core

was selected as a starting point for analysis as small scale premixed experiments could be conducted as could computational simulations. Existing simulation tools can calculate the maximum heat release (CEA2 Equilibrium) and the overall reaction rate (PSR) which together can be analyzed to classify a mixture from a thermodynamic and kinetic standpoint. Together, the thermodynamics and kinetics will directly control the effectiveness of a fire suppressant within a mixture and will determine whether the agent suppresses or enhances a fire in the premixed core.

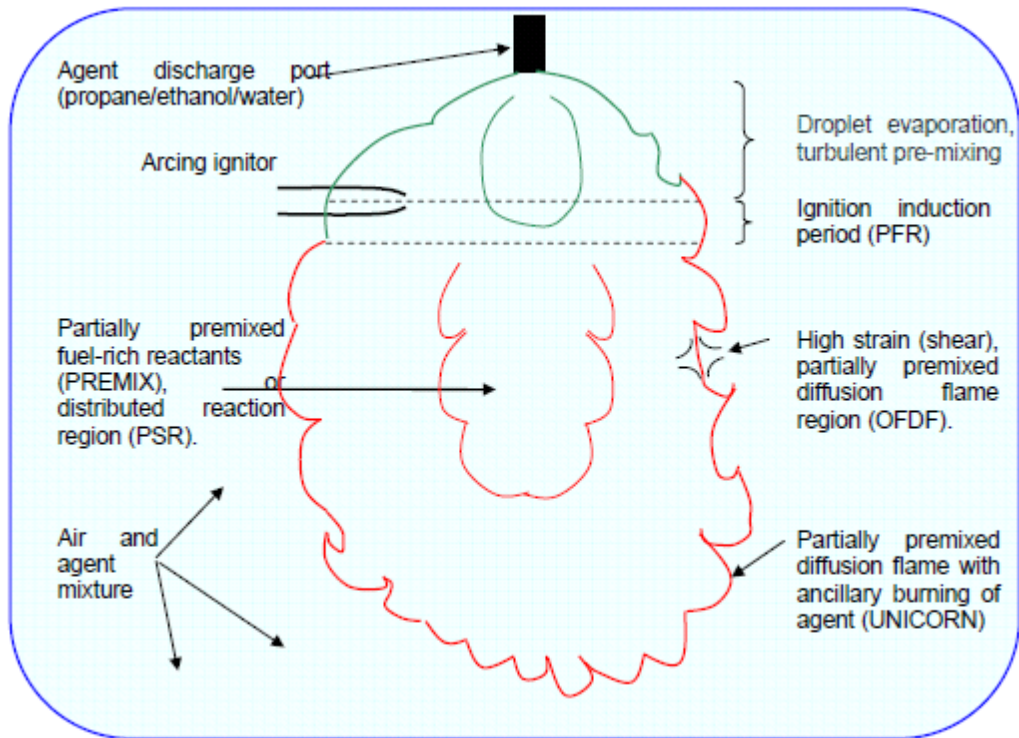


Figure 4: Illustration of simplified flame types present during aerosol can tests [20].

## 2.6 Description of Premixed Zone

The aerosol can test is a unique scenario where fuel is released at high pressure into an area of premixed air and fire suppressant. What is unknown is how well the contents of the aerosol can mix with the air and agent within the chamber. In order to examine a “premixed core” within the chamber where the air, agent, and aerosol can contents are premixed, a new

variable must be established that describes the volume of chamber which the released fuel mixes with. The chamber volume fraction ( $\eta$ ) has been introduced so that mixing can be varied in the experimental and computational analysis. Considering  $\eta$  as a variable makes it possible to map out all of the possible conditions that may have been present within the premixed zone during combustion in the FAA aerosol can tests.

The second variable that must be considered is the percentage of agent that is premixed with air inside the chamber before the aerosol can contents are released. This variable can be controlled so that the minimum concentration of suppressant can be determined. The percent agent within the chamber can also be varied to examine the effects of adding less than the minimum inerting concentration which is of particular interest when trying to determine a replacement suppression agent for aircraft cargo bays. Reinhardt [7] indicated that “since aircraft cargo compartment suppression agents may be present at subinerting design concentrations, because of stratification or larger than normal leakage, it is important that replacement agents be selected that do not increase the overpressure caused by an exploding aerosol can at concentrations below the inerting value.”

## **2.7 Converting FAA Chamber Mixtures to 2L Chamber Mixtures**

A full description of the weather on the days which Reinhardt performed the aerosol can tests had to be determined in order to perform comparable small scale experiments. Reinhardt did not document conditions such as the outdoor humidity or pressure. Data regarding the weather conditions at Atlantic City International Airport on the days the experiments were conducted was taken from Weather Underground archives and incorporated into Reinhardt’s summary of tests results [7] to create a spreadsheet that converted the concentration of each mixture component in the FAA aerosol can test premixed core to a volume fraction that could be

introduced into the 2 L chamber. The chamber volume fraction ( $\eta$ ) for which the contents of the aerosol can were assumed to mix with was left as a variable so that 2L chamber input concentrations could be determined for any amount of mixing within the FAA chamber. The introduction of weather details ensured the relative humidity of the mixture within the 2L chamber was equivalent to the relative humidity within the FAA chamber. The spreadsheet containing the weather information that was used to convert FAA chamber mixtures to 2L chamber mixtures is presented in Appendix 5. The relative humidity is shown in Figure 5 as a function of chamber volume fraction ( $\eta$ ) considered within the premixed zone. The relative humidity was found to be over 100% for mixtures contained in the 2L chamber with  $\eta$  values between 0 and 0.8. The humidity levels were due to the high water content contained within the aerosol can. In order for a mixture within the 2L chamber to be below supersaturation, over 80% of the chamber volume must be included with the aerosol can contents.

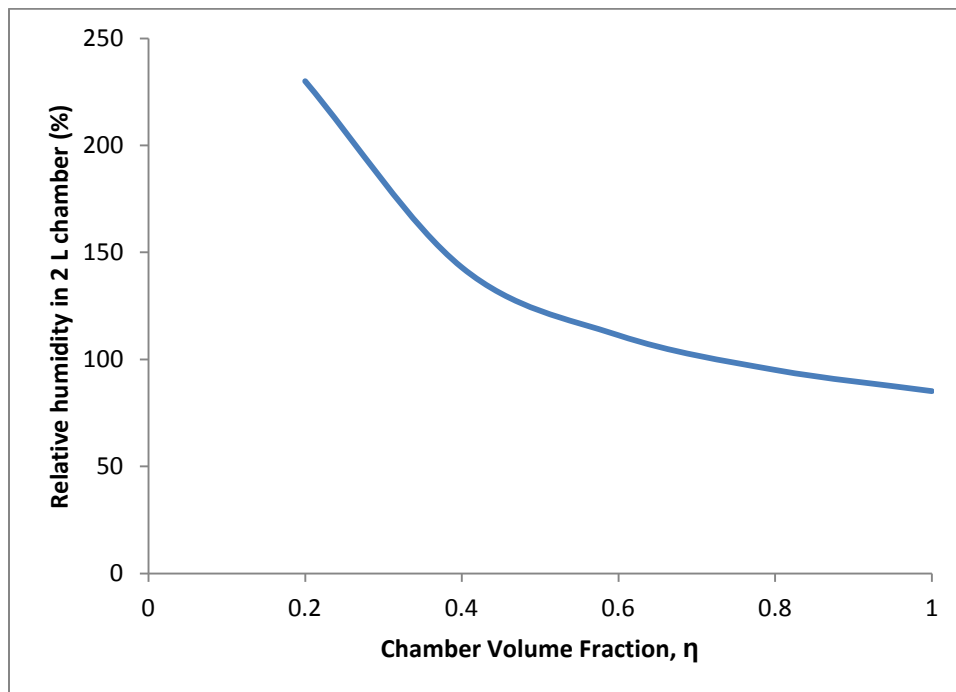


**Figure 5: 2L mixture relative humidity based on the chamber volume fraction ( $\eta$ ) assumed to mix with the aerosol can contents in the FAA chamber.**

## 2.8 Determination of Aerosol Can Fuel Equivalent (ACTe)

The ACT mixture used in the FAA tests was comprised of 5.87 moles of ethanol, 2.05 moles of propane, and 5.00 moles of liquid water [7]. Initially, tests conducted in the 2L chamber were done using this mixture as the fuel component. It was quickly determined that the addition of liquid reactants to the chamber was a challenging task based on the adsorbing nature of the stainless steel apparatus and the soot along the inner walls that may have been present within the chamber from prior tests. This made it difficult to determine the amount of ethanol and water present in vapor form within the mixture. The procedure for adding liquid reactants was to draw a vacuum in the chamber until the pressure was below 1 Torr. The Clausius-Clapeyron relation was then used to predict the vapor pressure of the liquid based on the chamber temperature. Water was added first due to its lower vapor pressure compared to ethanol. A given mass of water was obtained and injected into the chamber to produce the desired volume fraction in the final mixture. It was observed that after adding the water, the pressure within the chamber did not reach the partial pressure which was expected based on the Clausius-Clapeyron calculation. This was thought to be caused by water adsorption into the walls of the chamber as well as soot along the walls that formed from previous tests. The same phenomenon was observed when injecting ethanol into the chamber making it difficult to accurately measure the amount of liquid reactants present in the vapor phase within a mixture. Initially, the vapor pressures of water and ethanol were within 10% of the calculated values. As more tests were performed in the chamber the accuracy of the measured vapor pressures was reduced, with measured values 50% or more below the calculated values.

Due to the adsorbing nature of the chamber walls as well as the time required to clean the deposited soot off the walls after each test, a mixture was formulated to simulate the aerosol can

fuel. In order to create an aerosol can equivalent mixture (ACTe), properties of the aerosol can contents were matched including the adiabatic flame temperature and the carbon to hydrogen ratio. This yielded an equivalent mixture of 5.57 moles of propane and a relative humidity of 100% was used to simulate the contents of an aerosol can. A relative humidity of 100% was chosen for three reasons. First, high levels of saturation were required to match the hydrogen to carbon ratio. Second, Figure 5 showed that mixtures within the 2L chamber would be supersaturated for the majority of chamber volume fractions ( $\eta$ ) involved in the premixed zone. Finally, a relative humidity of 100% was chosen based on the inability to accurately insure a relative humidity other than 0% and 100%. It was known that some of the water injected into the chamber was going to be adsorbed which would have made it hard to run tests at any given relative humidity between 0% and 100%. Thus, a relative humidity of 100% could be achieved by adding extra water to the chamber and what was neither adsorbed nor vaporized would remain as liquid water. The liquid water was assumed to have a negligible effect on the reaction of the gaseous mixture.

Tests performed in the 2 L chamber were used to validate the simulated aerosol can fuel. The pressure rise resulting from mixtures containing the ACTe fuel was compared to the pressure rise for mixtures containing the actual ACT fuel for the same agent concentration and chamber volume fractions. The results of the tests performed for comparison can be seen in Table 4. Initial tests containing the aerosol can mixture were utilized in the comparison as the uncertainty in the vapor pressure values were below 10% for the earliest tests conducted in the 2L chamber. The error between the measured pressure rise is satisfactory considering the errors associated with partial pressure mixing and pressure measurements.

**Table 4: Peak pressure rise comparison of mixtures containing actual aerosol can fuel and ACTe fuel.**

% R125	Eta	ACT Mixture $\Delta P$ (bar)	Equip Mixture $\Delta P$ (bar)	% Difference
6.2	0.42	8.09	7.67	5.20
8.9	0.53	5.78	5.70	1.31
11	0.48	4.53	4.81	6.09

## 2.9 Relating Chamber Volume Fraction to Equivalence Ratio

By creating an ACTe fuel, tests were conducted with better accuracy with regard to mixture composition. Simplifying the aerosol can fuel also enabled the comparison of the chamber volume fraction involved in reaction ( $\eta$ ) to an equivalence ratio ( $\Phi$ ), which is a more familiar term used to describe flammable mixtures. Figure 6 presents the relationship between  $\eta$  and  $\Phi$  for mixtures containing no agent while also including the upper and lower flammability limits based solely on the volume percent of propane present within the mixture. Now, when tests are performed they can be viewed in terms of  $\eta$  for comparison to the FAA tests or in terms of  $\Phi$  so that results can be understood better based on a flammability standpoint. This relationship can also be helpful when deciding which values of  $\eta$  should be used for tests in the 2L chamber. Mixtures too far from the flammability window may be disregarded as potential test cases.

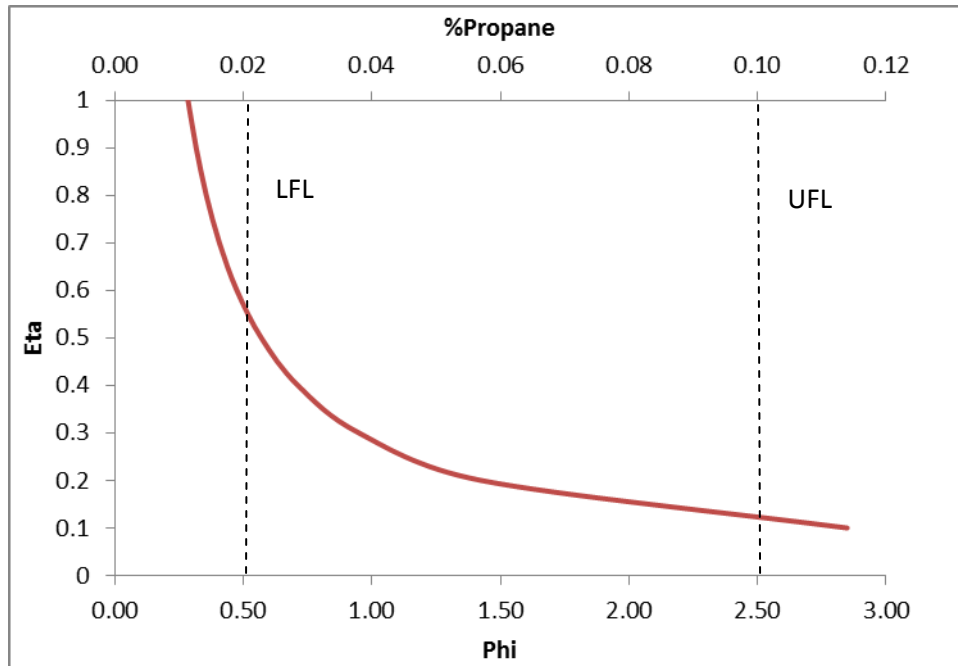


**Figure 6: Mixture equivalence ratio ( $\Phi$ ) based on the chamber volume fraction ( $\eta$ ) assumed to mix with ACTe fuel. The upper and lower flammability limits of the propane fuel component are also presented as bounds for which flammable mixtures are expected.**

When the equivalence ratio is stated for a mixture, it represents the value calculated based solely on the air required to oxidize the given amount of propane within the mixture. Water is then considered to have volume fraction of 2.5% which reduces the molar fractions of propane and air. Then, agent is added at a specified concentration which displaces only the air component of the mixture while the fuel and water molar fractions remain constant.



### 3. Computational Analysis

Computational analysis was performed to determine the effects of added agent on mixtures containing ACTe fuel and air. The various possibilities of mixtures that might exist in the premixed zone during the FAA test were classified based on the amount of chamber volume involved ( $\eta$ ) and the amount of agent added to the chamber. The mixtures were then viewed in terms of equivalence ratio ( $\Phi$ ) instead of chamber volume fraction ( $\eta$ ). The conversion was done so the effects of added agent could be easily comprehended by those not familiar with the FAA aerosol can test or the convention of determining mixture composition based on the chamber volume fraction involved in the premixed zone.

#### 3.1 Thermodynamic Equilibrium Calculations

Thermodynamics can be applied to determine the theoretical maximum amount of energy that can be released during a reaction based on the contents of the reactants. When a reaction is given infinite time to occur, the reactants are assumed to break down and reform into products that are considered most stable. Equilibrium can be applied and the maximum pressure and temperature rise can be calculated as well as the composition of the products. The thermodynamic equilibrium conditions of the aerosol can tests, with the ACTe fuel, were calculated using CEA2 of Gordon and McBride [21]. The software uses the method of minimizing the Gibbs free energy for a large number of species typically present in combustion reactions.

Constant volume (UV) equilibrium calculations were performed on ACTe fuel mixtures with various amounts of added agent. Halon 1301, HFC-125, and HCFC-123 were added at concentrations up to the minimum inerting concentration determined during the FAA tests. HCFC-123 was not subject to the FAA test, so as a conservative measure, the minimum inerting

concentration was assumed to be equal to that of HFC-125. Calculations were performed on an equivalence ratio basis so that the effects of added agent on mixture flammability could be studied. Appendix 6 presents the script used to compile and execute the CEA2 input files. The equivalence ratio was set for a given script which generated the mixture compositions and the mixture density. A text file containing the various percentages of agent to be added to the mixture was passed to the script file and the input files were assembled.

Calculations were performed with Halon 1301 added to ACTe fuel and air mixtures at concentrations up to 5%. Figure 7 presents the equilibrium final pressure as a function of equivalence ratio and percent Halon 1301. Each line represents a different equivalence ratio which can be converted into a given chamber volume fraction using Figure 7. For lean mixtures such as  $\Phi$  equal to 0.5, added suppressant only slightly increases the pressure rise from 6.65 bar with no agent to 7.44 bar with 5% agent. This is likely due to Halon 1301 having only one carbon atom that can react with oxygen in lean environments. Furthermore, it has been shown [5] that Halon does not have its own oxygen demand as the water produced from the hydrocarbon/air reactions supply enough O and H molecules necessary to oxidize Halon 1301. Overall, the lines representing each equivalence ratio are flat which shows that added Halon 1301 does not increase the heat release for lean mixtures.

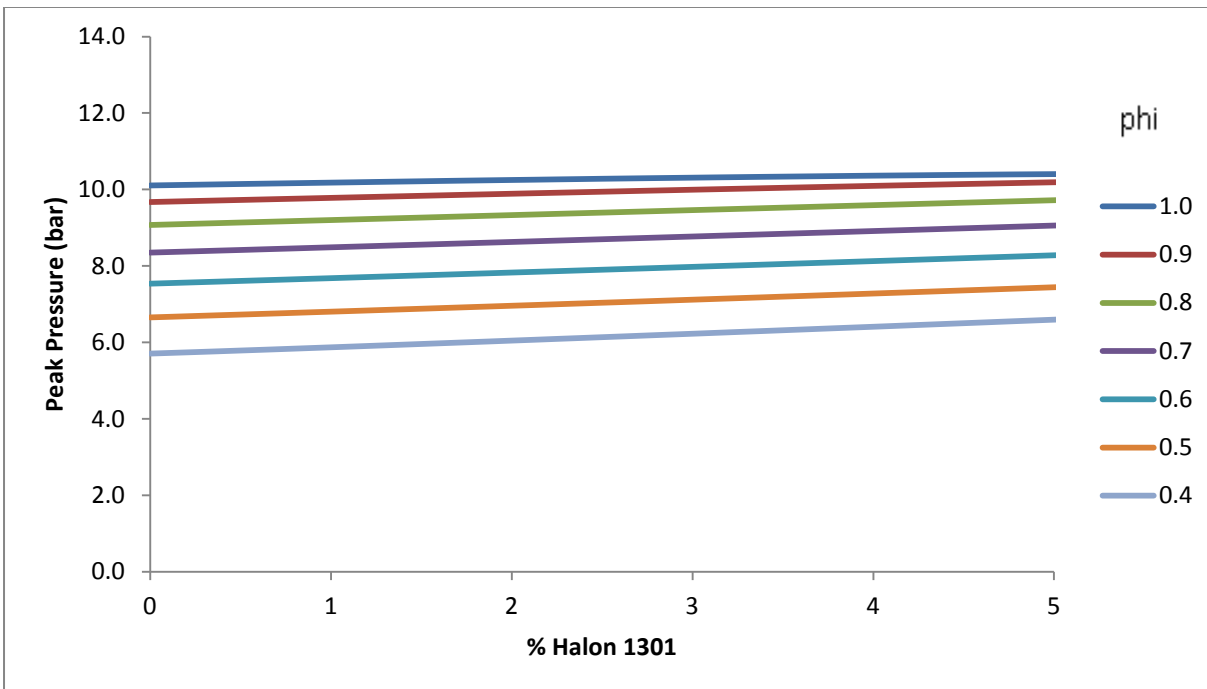


**Figure 7: Constant volume peak pressure for Halon 1301/air/ACTe mixtures as a function of percent Halon 1301 added in air for various mixture equivalence ratios ( $\Phi$ ).**

Calculations were performed with HFC-125 added to the ACTe mixture at concentrations up to 13.5%. Figure 8 presents the equilibrium final pressure as a function of equivalence ratio and volume percent of HFC-125 added to the mixture. The pressure rise of lean mixtures increases considerably as HFC-125 is added. The peak pressure rise occurs within the range of 5% to 9% HFC-125 for lean mixtures. For mixtures with an equivalence ratio ( $\Phi$ ) greater than 0.7 the pressure rise begins to fall as agent is added above the volume percent that produces peak pressure rise. For leaner mixtures the pressure rise levels out and remains near the peak value as more suppressant is added. Added HFC-125 was found to increase the pressure rise of lean mixtures by as much as 50% compared to the similar lean mixtures with no suppressant. The computational results for HFC-125 are consistent with the experimental results collected by Shebeko et al which showed that lean mixtures of  $H_2$  and  $CH_4$  with air can be promoted by adding fluorinated hydrocarbon inhibitors. Shebeko et al attributed promotion to

the additional heat release during the chemical conversion of the inhibitor [22]. This was consistent with the equilibrium calculations based on the observed equilibrium product compositions.

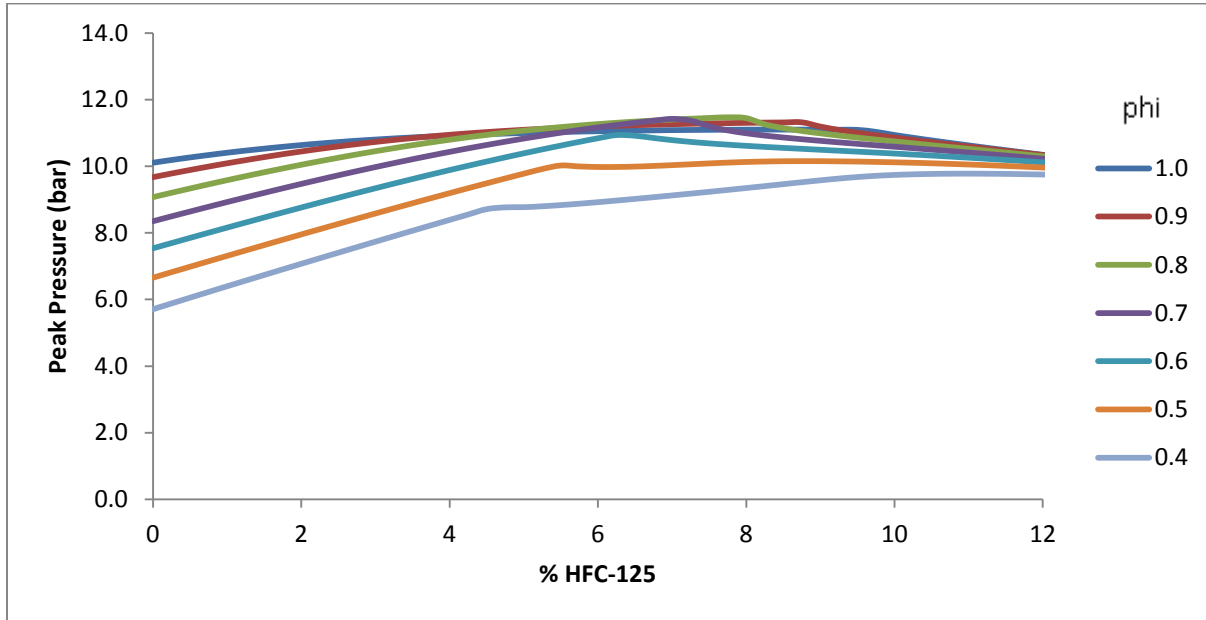


**Figure 8: Constant volume peak pressure for HFC-125/air/ACTe mixtures as a function of percent HFC-125 added in air for various mixture equivalence ratios ( $\Phi$ ).**

Similar constant volume calculations were performed with HCFC-123. Figure 9 shows the equilibrium pressure curves are similar to mixtures containing HFC-125. The peak pressure rise occurs at a slightly higher range of suppressant concentration between 8% and 10%. Added HCFC-123 was also found to increase the equilibrium pressure by as much as 50% for lean mixtures.

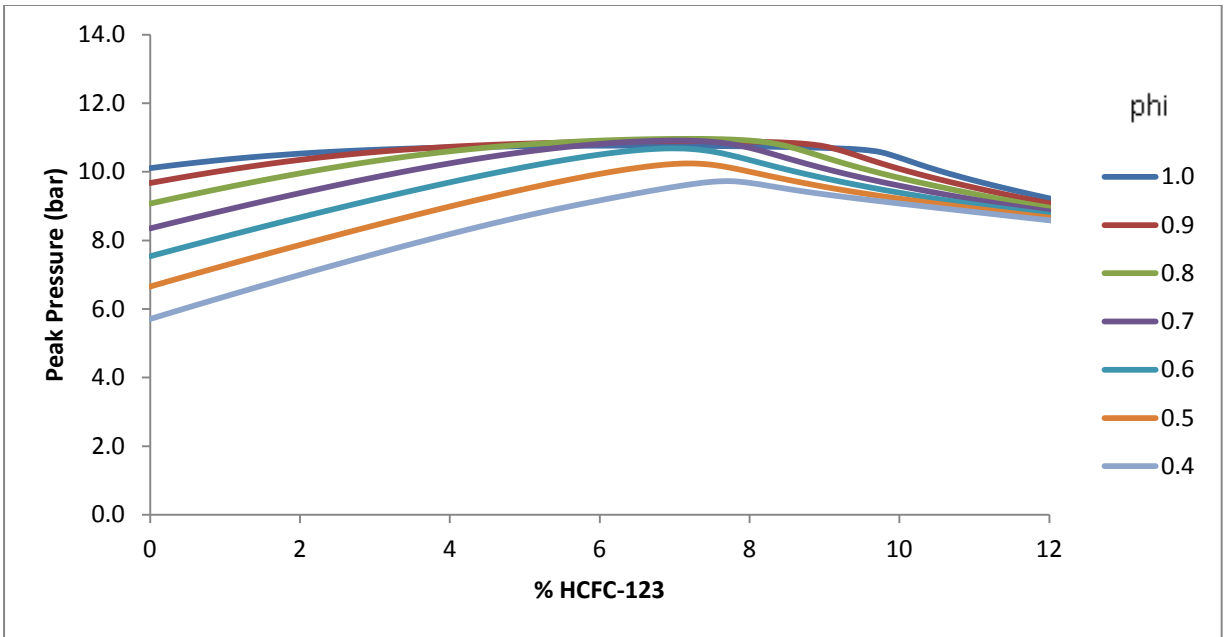


**Figure 9: Constant volume peak pressure for HCFC-123/air/ACTe mixtures as a function of percent HCFC-123 added in air for various mixture equivalence ratios ( $\Phi$ ).**

HCFC-123 was not studied in the FAA aerosol can test so the results of the constant volume equilibrium calculation were compared in Figure 10 to the results for mixtures containing HFC-125. The equivalence ratio values were limited to 0.7, 0.5, and 0.4 to reduce the number of plots on the figure and to highlight the differences under lean conditions. Overall, the thermodynamics of HCFC-123 are similar to HFC-125 as expected, based on the chemical similarity between compounds which contain the same number of hydrogen and carbon atoms which have the largest influence on heat release.

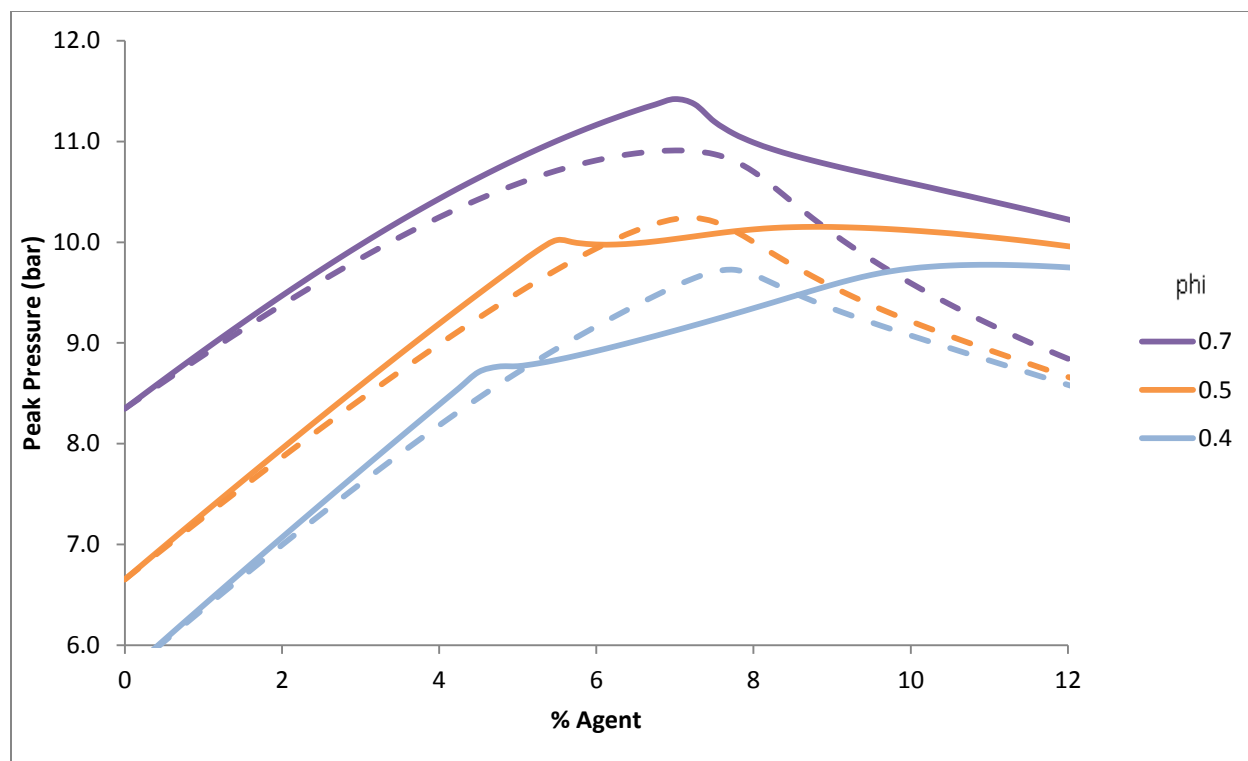


**Figure 10: Comparison of the peak pressure rise of mixtures containing HFC-125 (solid lines) and HCFC-123 (dashed lines) for an equivalence ratio ( $\Phi$ ) of 0.7, 0.5, and 0.4.**

### 3.2 Perfectly Stirred Reactor Calculations

The maximum heat release from equilibrium thermodynamics does not fully describe the reactions within the FAA ACT test as the reactants only have a finite amount of time to react before external effects such as heat loss occur. Flame extinction within the chamber is controlled by the Damkohler number which compares the flow residence time to the chemical time [19]. To consider the chemical time, the kinetics of a reaction can be studied to determine the overall reaction rate of a mixture. The thermodynamic analysis quantifies how the overall heat release changes as agent is added. Based on this analysis, HFC-125 and HCFC-123 would be better classified as fuels rather than suppressants. What must be understood is how these suppressants work. As active suppressants, they chemically alter the reaction pathways that occur within a mixture unlike passive suppressants that either displace oxygen or reduce temperature. Halogens

such as chlorine, fluorine, and bromine compete within the reaction zone to bond with radicals. By reducing radicals from the radical pool that would otherwise bond with other atoms, the reaction rate of a mixture is reduced. Overall, halogen atoms reduce radical formation and chain-branching, both of which decrease the rate of reaction. By studying the kinetics, a more comprehensive analysis can be made that may be able to help describe why HFC-125 causes overpressures in the FAA ACT test while Halon 1301 does not.

Perfectly stirred reactor (PSR) calculations were performed to determine the overall reaction rate of a mixture. A perfectly stirred reactor is an ideal reactor in which perfect mixing is achieved inside a control volume [23]. PSR calculations require an input file describing the mixture concentrations, residence time, and initial pressure. The reactor residence time,  $\tau$ , is defined as  $\tau = \rho V / \dot{m}$ , where  $\rho$  is the mixture density,  $V$  is the reactor volume, and  $\dot{m}$  is the mass flow rate. A chemical kinetic mechanism is also required as an input to describe the complete list of reactions that take place during combustion and the rate at which each reaction occurs. The governing equations of conservation of mass, species, and energy form a system of coupled non-linear algebraic equations [23] that are solved numerically using the SANDIA PSR code [24].

A script was used to generate input files and execute PSR calculations for a variety of equivalence ratios and agent concentrations. This script was similar to the script used to generate the equilibrium calculations. A separate script was used to iterate the calculations to determine the blow-out condition of a given mixture. A standard PSR calculation requires the input of residence time which is equivalent to the time in which the mixture is said to remain in the reactor. The final temperature of the mixture is given as an output, based on the time permitted for reactions to occur i.e. the residence time. As the duration of the residence time increases, the

final temperature approaches the adiabatic flame temperature calculated based on equilibrium. As the duration decreases, the final temperature decreases to a point where the mixture is not in the reactor long enough for any reaction to occur. The residence time just above the time where no reaction occurs is taken as the blow-out condition [20]. With the blowout condition known, the overall reaction rate ( $\omega_{\text{psr}}=1/\tau_{\text{blowout}}$ ) can be calculated.

To describe the reactions involving hydrocarbons, the four-carbon mechanism of Wang and co-workers, with 111 species and 784 elementary reactions was employed [25,26]. More detailed reactions of ethanol were added based on those of Dryer and co-workers [27-29], adding 5 species and 36 reactions. A modified version of the NIST HFC starting mechanism [30,31] was utilized to describe reactions of hydrofluorocarbons (HFCs) in hydrocarbon flames. Modifications were made based on recent experimental measurements and theoretical calculations. A complete description of the modifications was given by Linteris et al [20]. The modified HFC sub-mechanism adopted contained 51 species and 600 reactions. The sub-mechanism containing bromine was taken from the mechanism of Babushok et al [32, 33] to study reacting mixtures containing Halon 1301. The sub-mechanism added 10 species and 74 reactions. The final mechanism used during PSR simulations for mixtures containing either HFC-125 or Halon 1301 has 177 species and 1494 reactions.

For mixtures containing HCFC-123, the sub-mechanism describing the chemistry of C1-C2-chlorine containing species was taken from the work of Leylegian et al [34,35]. The block of reactions with C1-C2-species containing chlorine and fluorine atoms was adopted from the mechanism of Babushok et al [36]. The final kinetic model for inhibition includes 165 species and 1353 reactions. It is important to note that the mechanism of Babushok et al with C1-C2-species containing chlorine and fluorine atoms was recently developed. Minimal experimental



data exists for validation purposes so care must be taken when analyzing the results of PSR calculations using this mechanism.

PSR calculations were performed on mixtures containing ACTe fuel, air, and Halon 1301. Halon 1301 was added up to 5% by volume, which corresponded to the extinguishing concentration determined in the FAA tests [7]. Figure 11 presents the results for various mixture equivalence ratios ( $\Phi$ ). The results show that in no case does adding Halon 1301 to lean mixtures increase the overall reaction rate. For  $\Phi$  of 1.0, 0.9, and 0.8 the overall reaction rate ( $\omega_{psr}$ ) steadily decreases as more agent is added. For  $\Phi$  of 0.7, 0.6, and 0.5 the overall reaction rate steadily declines at first before dropping off sharply. For  $\Phi$  of 0.4 the overall reaction rate steadily declines at first before dropping off sharply.

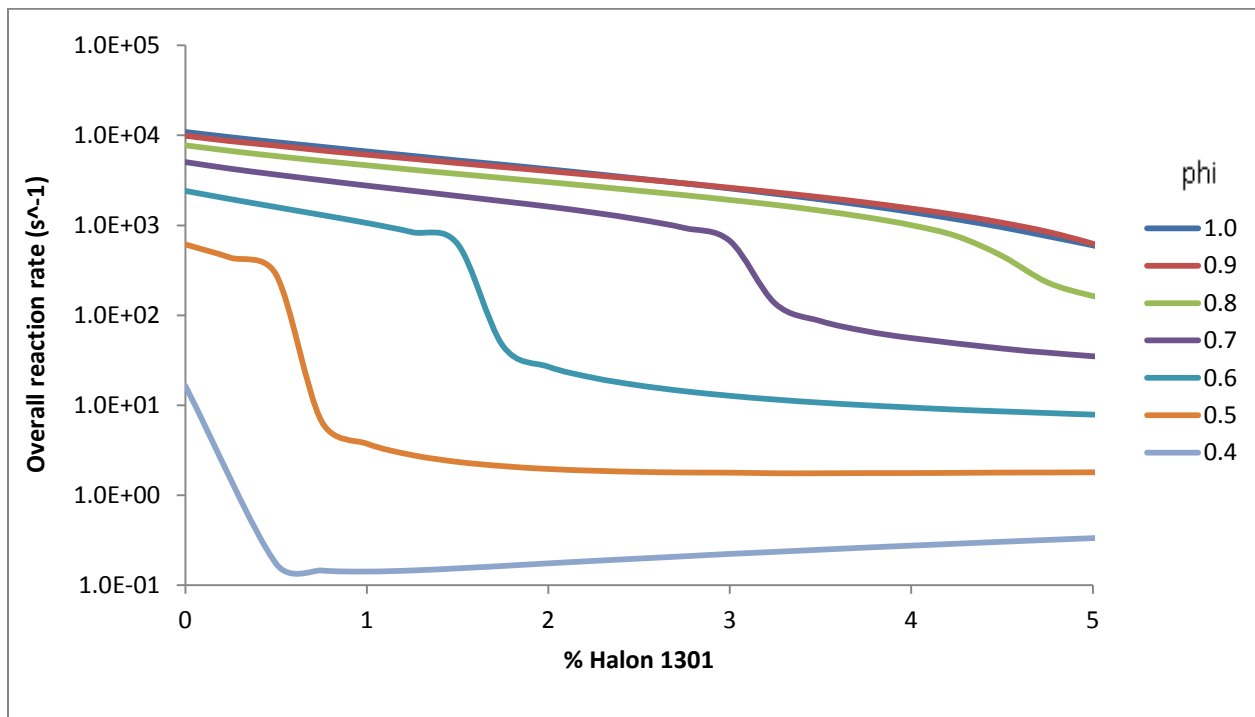
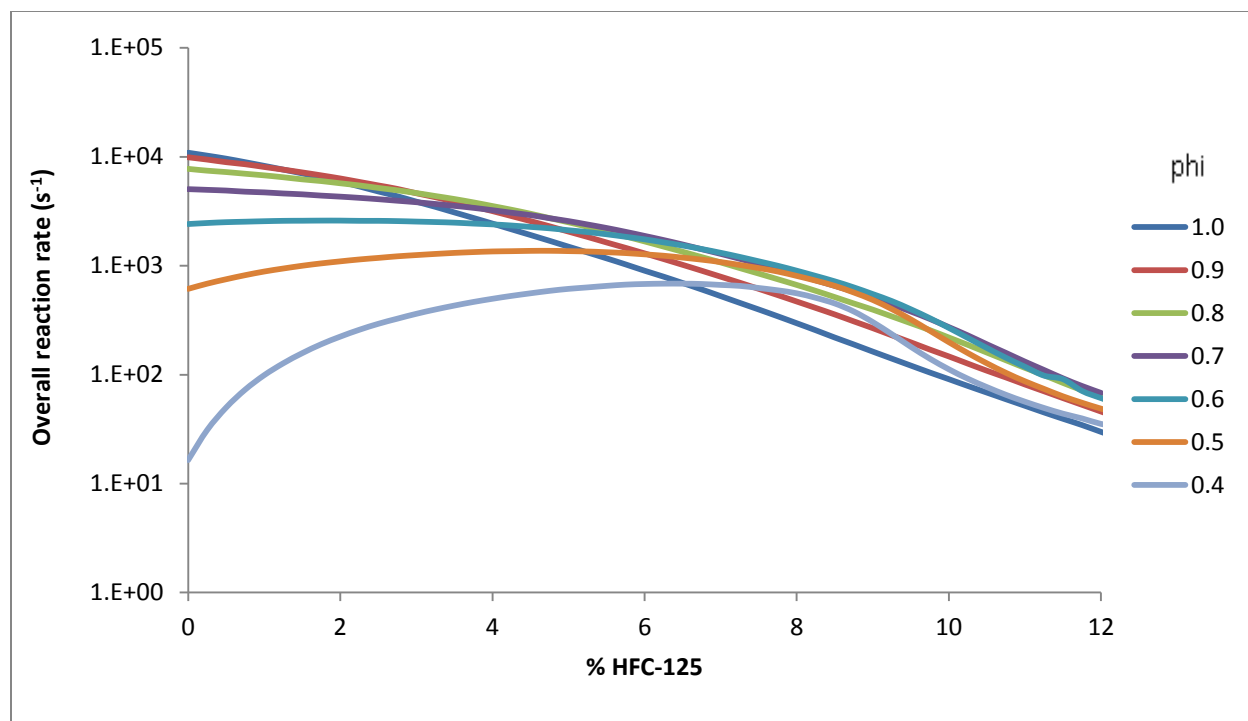


Figure 11: Overall reaction rate ( $\omega_{psr}$ ) for Halon 1301/air/ACTe mixtures as a function of percent Halon 1301 added in air for various mixture equivalence ratios ( $\Phi$ ).

PSR calculations were performed on mixtures containing ACTe fuel and HFC-125 at concentrations up to the minimum inerting concentration measured during the FAA tests [7]. Figure 12 presents the overall reaction rate as a function of the mixture equivalence ratio and the amount of agent added to the mixture. For  $\Phi$  between 1.0 and 0.7, the overall reaction rate decreases as agent is added with the maximum overall reaction rate occurring for mixtures without agent. For an  $\Phi$  of 0.6 the overall reaction rate remains unchanged as agent is added up to roughly 5%. Once more agent is added the overall reaction rate decreases. For even leaner mixtures the overall reaction rate actually increases as agent is added to the mixture. For an  $\Phi$  of 0.5 the overall reaction rate ( $\omega_{psr}$ ) is  $613 \text{ s}^{-1}$  with no added agent. The overall reaction rate doubles at an agent concentration of 4.75% to  $1370 \text{ s}^{-1}$ . The increase is even larger when  $\Phi$  is 0.4. The overall reaction rate increases from  $16 \text{ s}^{-1}$ , with no agent, to  $685 \text{ s}^{-1}$  at an agent concentration of 6.25%. This shows that when added to lean mixtures at sub-inerting concentrations, HFC-125 enhances the burning rate.



**Figure 12: Overall reaction rate ( $\omega_{psr}$ ) for HFC-125/air/ACTe mixtures as a function of percent HFC-125 added in air for various mixture equivalence ratios ( $\Phi$ ).**

PSR calculations were performed on mixtures containing HCFC-123. The minimum inerting concentration of HCFC-123 in the FAA aerosol can test was unknown so calculations were performed with a maximum agent concentration equal to the minimum inerting concentration of HFC-125. Figure 13 presents the overall reaction rate for the range of mixtures that may exist in the premixed zone of the FAA aerosol can test. The overall reaction rate ( $\omega_{psr}$ ) declines steadily when  $\Phi$  is between 1.0 and 0.6. For  $\Phi$  equal to 0.5, the overall reaction rate decreases as agent is added up to 2%, then flattens out up to an agent concentration of about 7.5% before decreasing again. For  $\Phi$  equal to 0.4, the overall reaction rate increases from  $16 \text{ s}^{-1}$  to  $31 \text{ s}^{-1}$  at an agent concentration of 6%. That is much less of an increase when compared to mixtures containing HFC-125 which start out at the same initial overall reaction rate but increases to  $685 \text{ s}^{-1}$  as the agent concentration reaches 6.25%.

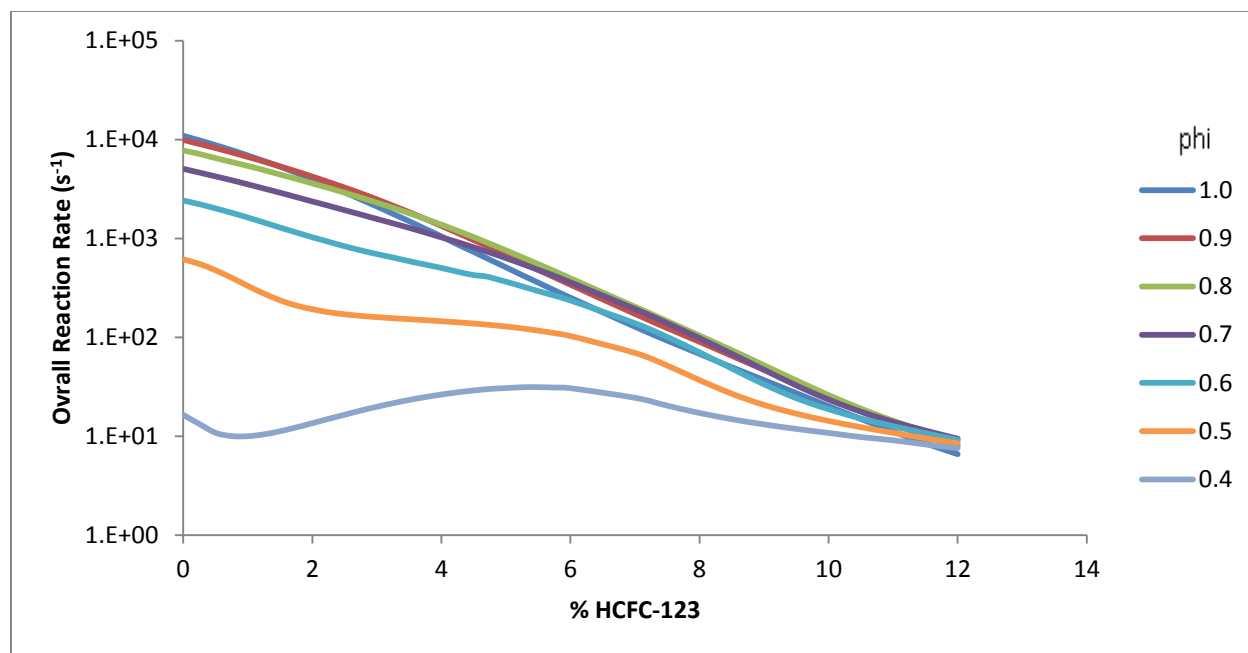


**Figure 13: Overall reaction rate ( $\omega_{psr}$ ) for HCFC-123/air/ACTe mixtures as a function of percent HCFC-123 added in air for various mixture equivalence ratios ( $\Phi$ ).**

The HCFC-123 PSR results were compared in Figure 10 to the results for mixtures containing HFC-125. The equivalence ratio values were limited to 0.7, 0.5, and 0.4 to reduce the number of plots on the figure and to highlight the differences under lean conditions. The simulations show that mixture containing HCFC-123 have lower overall reaction rate compared to mixtures containing HFC-125. For  $\Phi$  equal to 0.5 adding HFC-125 increase the overall reaction rate while adding HCFC-123 decreases the reaction rate when compared to mixtures containing no agent. For  $\Phi$  equal to 0.4 the overall reaction rate substantially increases with added HFC-125 and stays relatively flat when HCFC-123 is added.

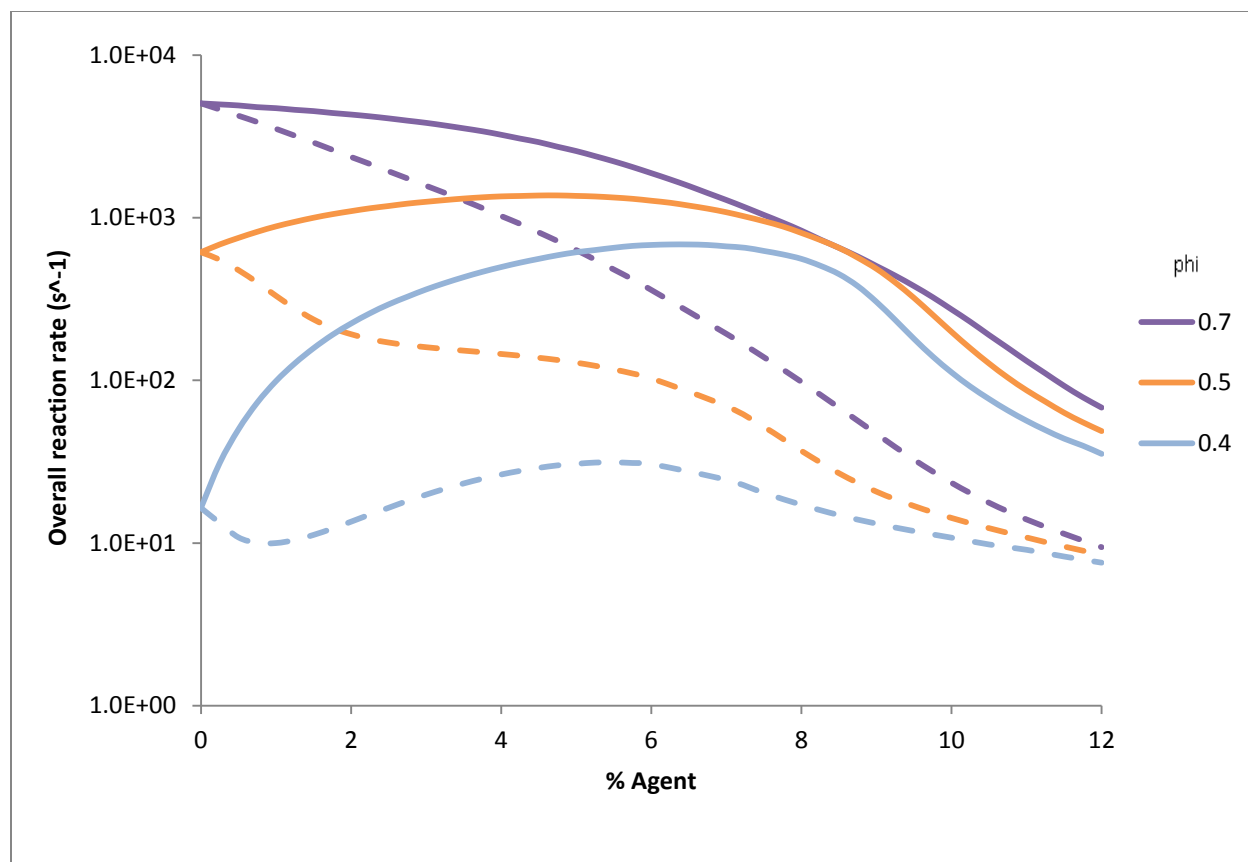


**Figure 14: Comparison of the overall reaction rate ( $\omega_{psr}$ ) of mixtures containing HFC-125 (solid lines) and HCFC-123 (dashed lines) for an equivalence ratio ( $\Phi$ ) of 0.7, 0.5, and 0.4.**

HCFC-123 may potentially perform better than HFC-125 in the aerosol can test based on kinetics. From the thermodynamic analysis the addition of HCFC-123 at sub-inerting concentrations should have the same effect as HFC-125 on the peak pressure rise. If the kinetics are slowed enough then the added heat release of HCFC-123 may not be an issue. The pressure rise in the chamber may be reduced regardless of the calculated heat release as less of the premixed core will have time to react before heat losses and quenching help to extinguish the flame. Kinetic simulations show a reduction in the overall reaction rate as HCFC-123 is added to lean mixtures but the required reduction necessary to reduce the amount of premixed core that reacts in the FAA chamber is unknown. The beauty of Halon 1301 is that the kinetics are slowed as agent is added, but even if they are not slowed enough to extinguish the flame, the

heat release of the mixture does not increase with the addition of Halon 1301 at any concentration below the minimum inerting concentration. HCFC-123 does not have the ideal thermodynamic properties like Halon 1301, but the kinetic effects are an improvement over HCF-125. To determine if the reduction in the overall reaction rate for mixtures containing HCFC-123 will help at sub-inerting concentrations, small scale experiments have been performed.

## **4. Experimental Results**

Laboratory scale experiments were designed to meet the following objectives:

1. Provide experimental evidence to support the computational results.
2. Determine if the supersaturated environment of the aerosol can test may have influenced the suppression effectiveness of HFC-125.
3. Determine the amount of nitrogen required for a dual HFC-125/nitrogen system to pass the aerosol can test.
4. Determine if HCFC-123 may be a better alternative than HFC-125 in cargo bay suppression systems based on suppression performance.

Careful selection of experimental mixtures has allowed for the four objectives to be studied simultaneously while performing minimal 2L chamber experimental runs.

### **4.1 Determination of Experimental Mixtures**

During the FAA aerosol can tests, a premixed core is assumed to form. The composition of the core is highly dependent on how well the contents of the aerosol can mix within the chamber. Due to the unknown amount of mixing, a wide range in core composition is considered to be possible within the chamber. When performing laboratory scale tests not all mixture compositions can be tested based on time restraints so careful selection of experimental mixtures is crucial. Experimental mixtures were selected based on the following criteria:

1. Select mixtures that can be compared to the FAA test results.
2. Select mixing that roughly corresponds to the mixing predicted in the FAA tests.
3. Select mixtures that can be compared to the computational results.

4. Select mixtures preferably at the same chamber volume fraction to reduce the number of variables so that the pressure rise results from tests with different agent concentrations are comparable.

The mixtures testing in the 2 L chamber were comprised of ACTe fuel, air, and agent. The agent concentrations considered were 6.2%, 8.9%, and 11.2% to be consistent with the sub-inerting concentrations tested during the FAA tests [7]. Figure 15 provides the estimated chamber volume fraction ( $\eta$ ) involved for mixtures containing HFC-125 in the aerosol can test [37]. The estimates are based on  $\eta$  that produces the peak adiabatic flame temperature from thermodynamic equilibrium calculations. The chamber volume involved ( $\eta$ ) when 6.2% agent was added to the chamber is around 0.42. For 8.9% agent,  $\eta$  is 0.5 and for 11.2%,  $\eta$  is roughly 0.71. Although the chamber volume fraction ( $\eta$ ) ranges from 0.42 to 0.71,  $\eta$  of 0.5 was chosen for all agent concentrations to fulfill the selection criterion of having a similar  $\eta$  value for all tests. Variation in  $\eta$  from one agent concentration to another would make comparing the experimental results difficult. Lastly, choosing  $\eta$  of 0.5 gives a mixture equivalence ratio ( $\Phi$ ) of 0.57, which is slightly above the lean limit for propane/air mixtures. This allows the results to be compared to the computational results that were performed for lean mixtures. The most interesting computational results for mixtures containing HFC-125 were at lean conditions ranging from an equivalence ratio ( $\Phi$ ) of 0.4 to 0.6.



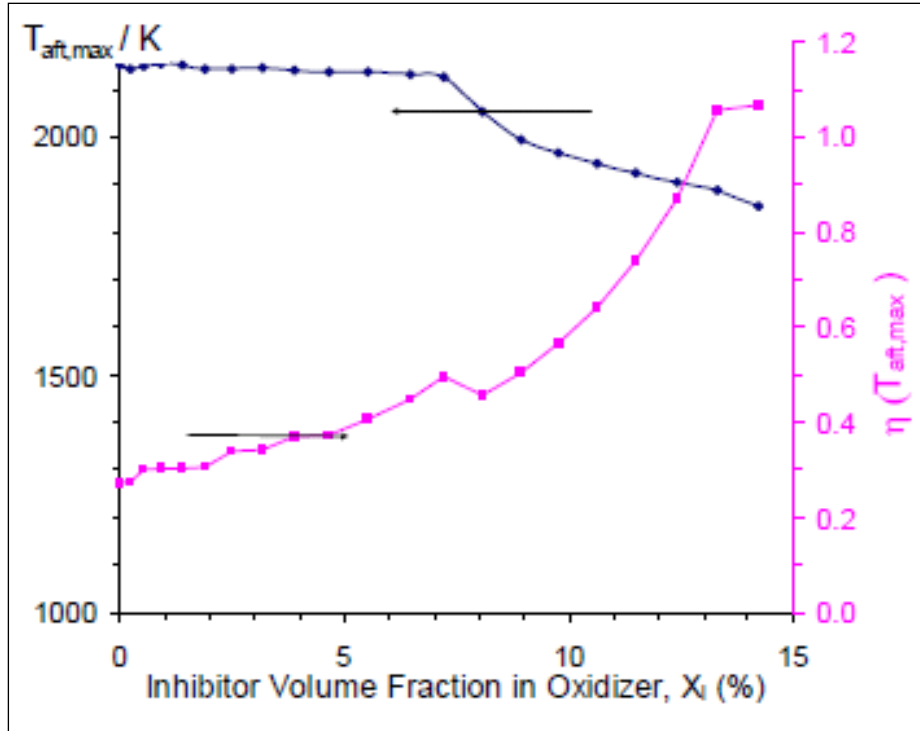


**Figure 15: Chamber volume fraction (pink) that produces the peak adiabatic flame temperature (blue) for mixtures containing the actual aerosol can contents and HFC-125 [37].**

2 L chamber tests were devised to study the effects of water vapor on mixtures with agent concentrations and volume fractions mentioned previously. Tests were performed on mixtures with a relative humidity of 0% and 100%. The ACTe mixture contains water at a relative humidity of 100% to match the high levels of saturation that exist for mixtures consisting of a wide range of  $\eta$ . Mixtures containing the same ratio of propane, air, and agent were studied with the water portion removed to form mixture with a relative humidity of 0%. Tests were also performed over a range of oxygen in air. This was accomplished with nitrogen dilution. Tests were performed in standard air with 21% oxygen and in air containing 20% and 19% oxygen. Table 2 summarizes the 12 tests that were conducted with HFC-125.

**Table 5: Summary of tests conducted with a chamber volume fraction ( $\eta$ ) of 0.5 ( $\Phi=0.57$ ) with various relative humidity and oxygen concentrations.**

$\eta=0.5$			
$\Phi=0.57$			
Agent Peak Concentration (%)	Relative Humidity (%)	Oxygen Vol Fraction	F/H
6.2	0	0.21	1.22
6.2	100	0.21	1.01
6.2	100	0.20	1.01
6.2	100	0.19	1.00
8.9	0	0.21	1.59
8.9	100	0.21	1.34
8.9	100	0.20	1.33
8.9	100	0.19	1.32
11.2	0	0.19	1.85
11.2	100	0.21	1.55
11.2	100	0.20	1.56
11.2	100	0.19	1.57

#### **4.2 Relating 2L Chamber Pressure Rise to FAA Chamber Pressure Rise**

Tests were conducted in the 2 L chamber to study the suppression performance of HFC-125 and HCFC-123 on mixtures containing ACTe fuel and air. Mixtures were introduced into the chamber and given time to mix so that they were representative of a premixed core that was hypothesized, by Linteris et al [20], to exist within the FAA chamber after the contents of the aerosol can were released. The pressure rise within the 2 L chamber is representative of the pressure rise within the premixed zone in the FAA test. The 2 L pressure rise can be compared to overall pressure rise in the FAA chamber by assuming the premixed zone undergoes combustion and the remaining chamber volume contents do not react and remain at the initial temperature. By doing so, the pressure rise of the premixed zone can be converted into an equivalent volume expansion, given the pressure was held constant, using the ideal gas law

$(P_f/P_i=V_f/V_i)$ . Then, the volume of the reacted zone can be added to the volume of the non-reacted zone. This total volume can be converted back to a final pressure rise, assuming the volume was held constant, using the ideal gas law once again. Similar work was performed by Linteris et al [37] but with one small change. This technique was used to relate constant pressure equilibrium results to the FAA pressure rise. The first step of converting pressure rise to volume expansion was not performed by Linteris et al as the equilibrium calculations were performed at constant pressure.

### **4.3 Test Results for HFC-125**

Measured 2L chamber peak pressure rise for mixtures containing 21% oxygen in air were compared to measured pressure rise in the FAA chamber as an extra check on the validity of the mixing assumption and the ACTe fuel assumption. Table 6 presents the FAA chamber pressure rise for tests with added agent, the estimated pressure rise within the FAA chamber based on the 2L chamber experimental pressure rise, and the error between the two values. The experimental pressure rise measurements for mixtures containing sub-inerting concentrations of HFC-125 were consistent with the overpressures observed in the FAA aerosol can test with the largest error occurring at an HFC-125 concentration of 11.2%. The discrepancy is likely caused by the selection of a chamber volume fraction ( $\eta$ ) of 0.5 while it was predicted that a  $\eta$  of 0.71 was required to reach the overpressure measured in the FAA test. It should be noted that experiments were conducted with 11.2% HFC-125 with a chamber volume fraction of 0.71 and the peak 2L chamber pressure rise was 0.70 bar which resulted in an predicted FAA chamber pressure rise of 0.50 bar. This was less than the estimated FAA chamber pressure rise when  $\eta$  was taken to be 0.5. This shows that some other influence such as compressive heating is contributing to the pressure rise when 11.2% HFC-125 is added to the FAA chamber.

**Table 6: Comparison of FAA chamber pressure rise to the predicted pressure rise based on peak pressure measured in 2L chamber.**

% HFC-125	FAA $\Delta P$ (bar)	Experimental FAA $\Delta P$ (bar)	% Error
0	1.68	1.91	13.68
6.2	3.59	3.53	1.57
8.9	3.65	3.02	17.26
11.2	3.59	2.31	35.66

#### **4.3.1 Effects of Water Vapor on Peak Pressure Rise**

It was observed by Takizawa et al that adding water to fluorocompounds with an F/H ratio greater than unity enhanced the flammability range as water vapor participates in the combustion reaction by supplying hydrogen atoms [38]. Gmurchyk et al found that the F/H ratio in the total reactants has a significant effect on the extinguishing concentrations of HFCs for C<sub>2</sub>H<sub>4</sub>/air flames under highly dynamic conditions [39]. Due to the high saturation levels found in mixtures within the FAA chamber the effect of water vapor on the peak pressure rise of mixtures containing HFC-125 was examined to determine if water vapor is contributing to the observed overpressures.

Measured pressure rise for the experiments conducted in the 2 L chamber is presented in Figure 16. The addition of water vapor substantially increased the pressure rise for mixtures containing 8.9% and 11.2% agent. The increase in pressure rise was less pronounced for mixtures containing 6.2% agent. This is likely due to a fluorine to hydrogen ratio (F/H) greater than unity for mixtures containing 8.9% and 11% agent while mixtures containing 6.2% agent exhibit an F/H ratio closer to unity.

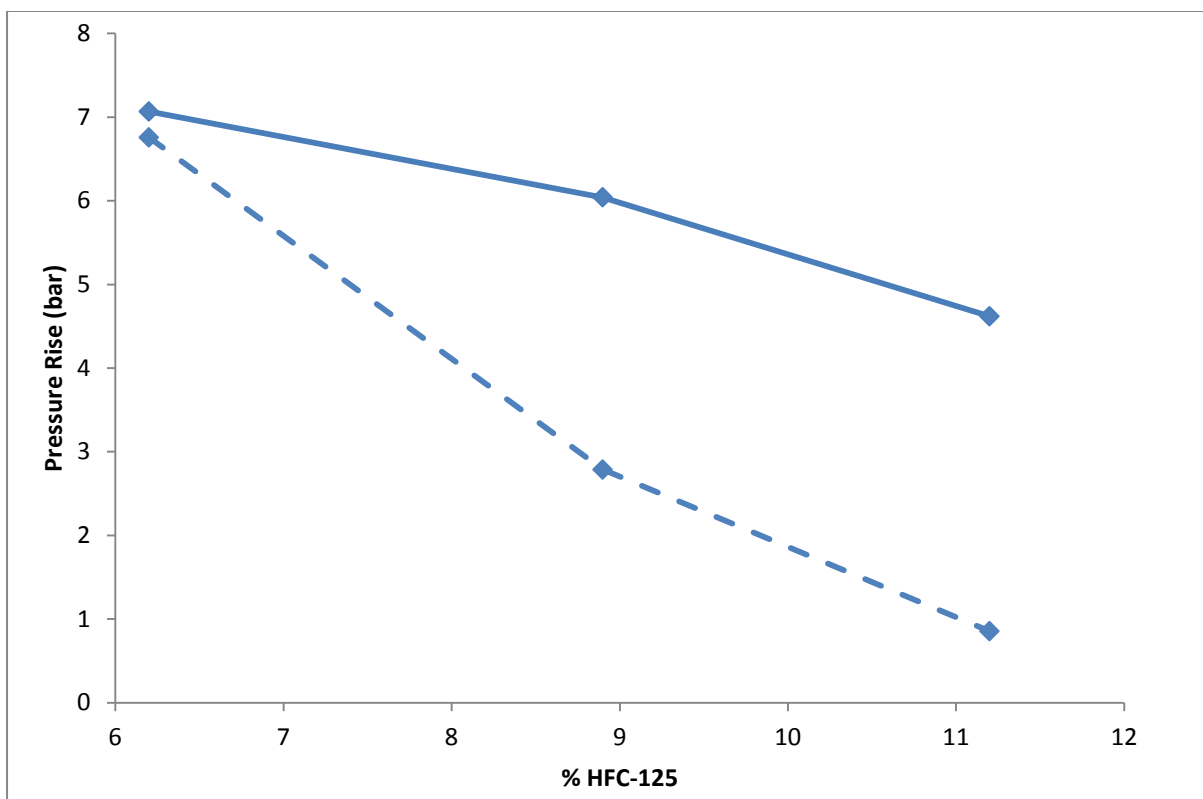


**Figure 16: Peak pressure rise in 2 L chamber for mixtures containing ACTe fuel, air, and HFC-125 with a relative humidity of 100% (solid line) and a relative humidity of 0% (dotted line). The chamber volume fraction involved ( $\eta$ ) is 0.5.**

For analysis, CEA2 and PSR calculations were performed at each test condition to study how HFC-125 and water vapor concentrations affect the adiabatic flame temperature. The adiabatic flame temperatures determined by CEA2 equilibrium calculations are presented in Figure 17. As the agent concentration increases from 6.2% to 11.2% the adiabatic flame temperature decreases by roughly 200K for mixture containing a relative humidity of 0% and 100%. The effect of water vapor on adiabatic flame temperature appears to be negligible, only increasing the temperature by 111 K, 13 K, and 3 K, for 6.2%, 8.9%, and 11.2% agent concentrations respectively.

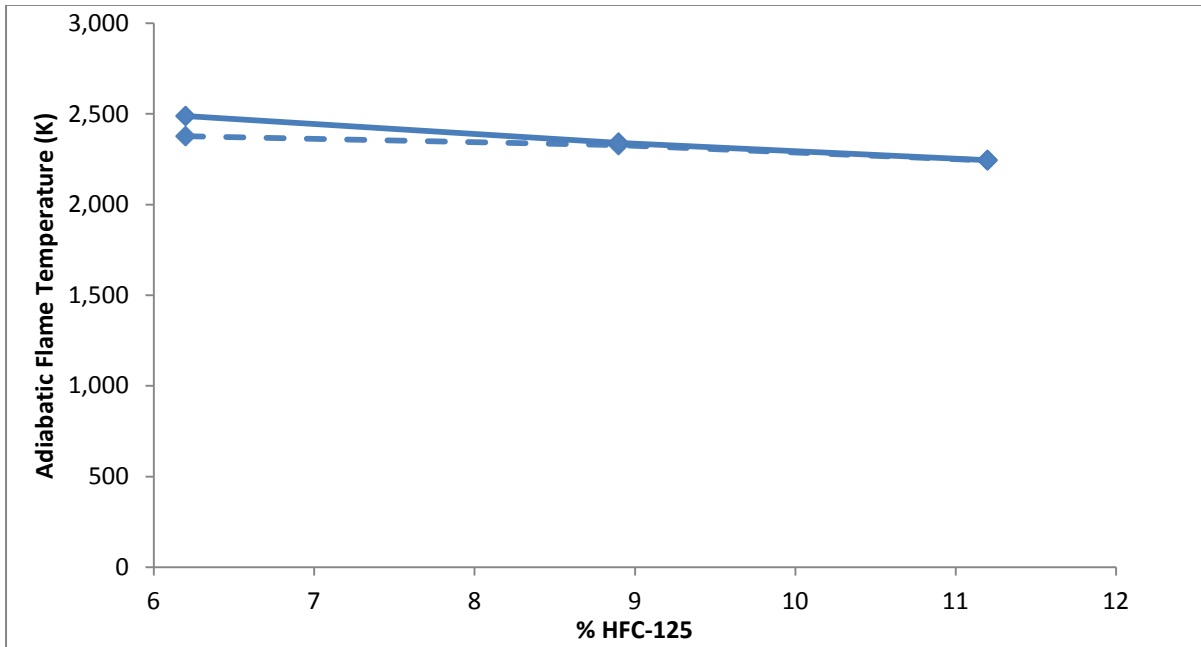


**Figure 17: Equilibrium adiabatic flame temperature for mixtures containing ACTe fuel, air, and HFC-125 with a relative humidity of 100% (solid line) and a relative humidity of 0% (dotted line). The chamber volume fraction involved ( $\eta$ ) is 0.5.**

The overall reaction rate obtained from PSR calculations is presented in Figure 18. Agent concentration had the strongest influence on  $\omega_{\text{psr}}$ . The reaction rate for mixtures containing 6.2% agent was about  $1000 \text{ s}^{-1}$  while it was closer to  $50 \text{ s}^{-1}$  for mixtures containing 11.2% agent. Water vapor was found to increase  $\omega_{\text{psr}}$  by a factor of 2.5 for mixtures containing 8.9% agent and by a factor of 2.8 for mixtures containing 11.2% agent. Added water vapor did not have any effect on  $\omega_{\text{psr}}$  for mixtures containing 6.2% agent due to an F/H ratio at or below 1 for both cases.

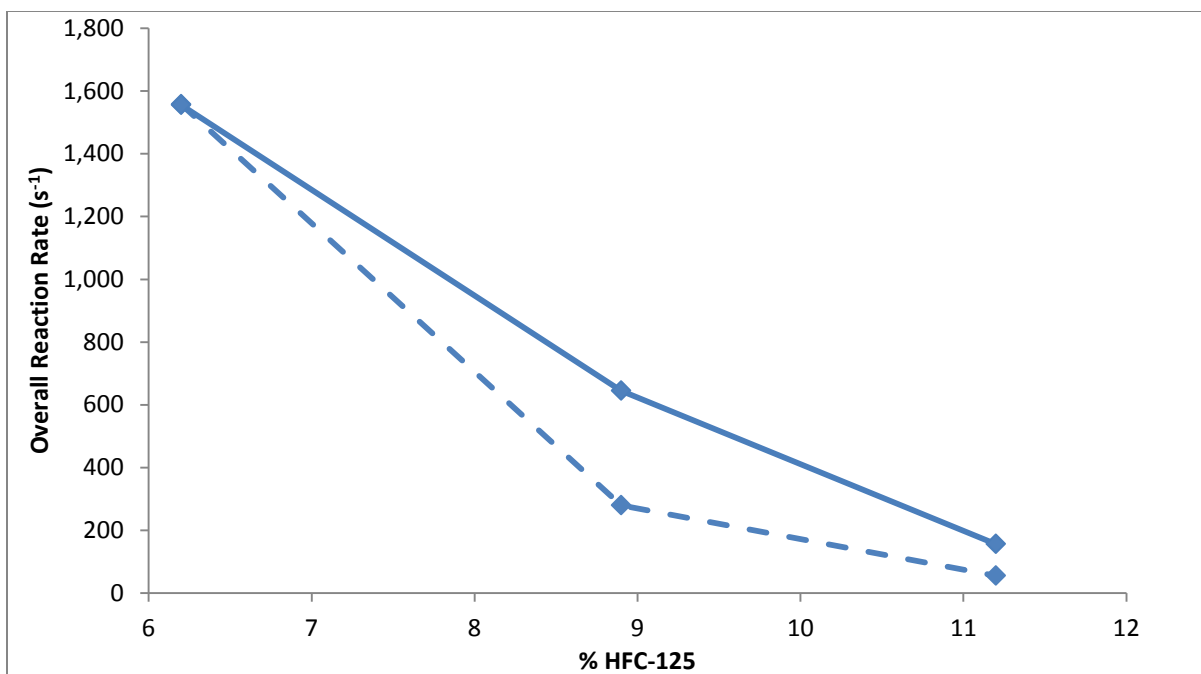


**Figure 18: Perfectly stirred reactor prediction of the overall reaction rate for mixtures containing ACTe fuel, air, and HFC-125 with a relative humidity of 100% (solid line) and a relative humidity of 0% (dotted line). The chamber volume fraction involved ( $\eta$ ) is 0.5.**

#### 4.3.2 Effect of Nitrogen Dilution on Peak Pressure Rise

The goal of testing mixtures with nitrogen dilution was to find the concentration that eliminates the overpressure for mixtures containing sub-inerting concentrations of HFC-125. For comparison purposes, the pressure rise observed during FAA aerosol can tests without added agent was reviewed. Two runs were performed that yielded an average peak pressure rise of 1.68 bar. The FAA chamber pressure rise can be converted into a 2L pressure rise based on the amount of chamber volume ( $\eta$ ) assumed to be involved in mixing. With a chamber volume fraction ( $\eta$ ) of 0.5 the expected pressure rise in the 2L chamber was found to be 3.36 bar. This is a general comparison which can be used during testing as a benchmark for the maximum pressure rise that can occur within the 2 L chamber without causing overpressure in the FAA chamber. An alternative comparison was proposed based on the 2L pressure rise of a mixture with no added agent and a chamber volume fraction ( $\eta$ ) equal to 0.5. If the chamber volume

fraction involved is similar for two mixtures then the final pressure in the FAA chamber is only a function of the pressure rise in the premixed zone which is equivalent to the mixture tested in the 2L chamber. Based on the simplified analysis, the remaining volume is assumed to be inert regardless of its composition i.e. whether or not it contains agent. The measured peak pressure rise in the 2L chamber for the mixture without HFC-125 was 3.82 bar. The two methods of determining the criterion for whether measured peak pressures in the 2L chamber would produce overpressures in the FAA aerosol can tests yielded slightly different maximum allowable pressures. The maximum peak pressure for mixtures containing HFC-125 was set at 3.36 bar which was taken from the FAA aerosol can tests data which was also the lesser of the two calculated values.

Mixtures containing 21%, 20%, and 19% oxygen in air were tested in the 2 L chamber to study the effects of nitrogen dilution on peak pressure rise. Peak pressure rise of the nine mixtures containing ACTe fuel, air, and HFC-125 is presented in Figure 19 as a function of HFC-125 concentration. The line colors represent a volume fraction of oxygen contained in air. 21%, 20%, and 19% are colored blue, red, and green respectively. The dotted black line represents the peak pressure rise (3.36 bar) that can occur within the 2L chamber without causing an overpressure in the FAA chamber. Any pressure rise above the black dotted line would be considered a failure in the aerosol can test.

It was found that nitrogen dilution resulting in 19% oxygen in air was not sufficient in reducing the peak pressure rise measured in the 2L chamber. Nitrogen dilution must reduce the peak pressure rise of mixtures containing 6.2% HFC-125 by almost half. This was not the case as the pressure was reduced by 1.31 bar, or 19%. The largest reduction in peak pressure rise occurred for mixtures containing 8.9% HFC-125. The pressure rise was reduced from 6.04 bar



to 3.84 bar which was a 36% reduction. Nitrogen dilution resulting in 19% oxygen in air successfully reduced the peak pressure of mixtures containing 11.2% HFC-125. The peak pressure went from 4.62 bar to 3.03 bar which is below the maximum pressure rise allowable.

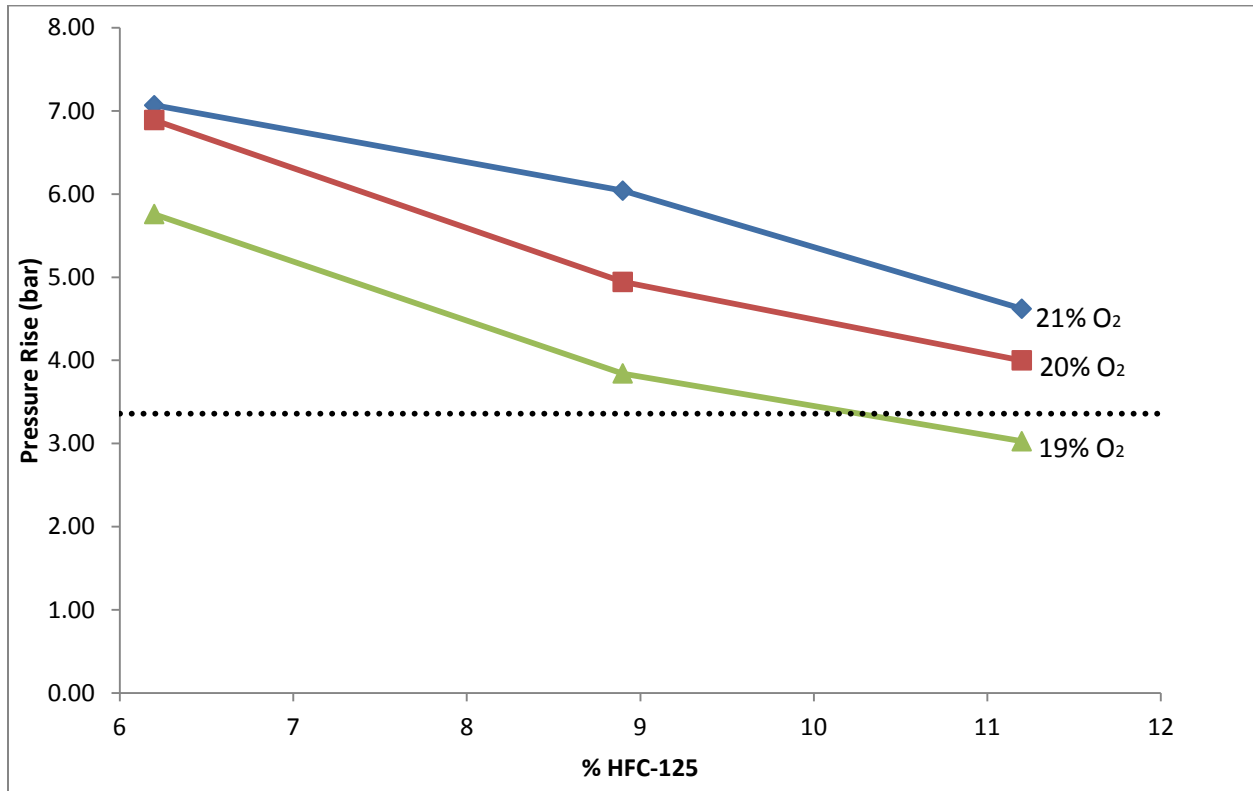


**Figure 19: Peak pressure rise of HFC-125 mixtures containing 21%, 20%, and 19% oxygen in air. The chamber volume fraction involved ( $\eta$ ) is 0.5. The horizontal dotted line represents the maximum allowable peak pressure in the 2L chamber that will not create an overpressure in the FAA chamber.**

#### 4.4 Test Results for HCFC-123

Experiments were performed in the 2 L chamber with mixtures containing ACTe fuel, air, and HCFC-123. The mixtures tested were similar to the HFC-125 mixtures with respect to agent concentrations and  $\eta$ , with HCFC-123 replacing HFC-125 as the suppressing agent. HCFC-123 was not considered in the FAA aerosol can test so mixtures have been selected to allow for direct quantitative comparison of the small scale HCFC-123 results to the HFC-125 results. Agent concentrations of 6.2%, 8.9%, and 11.2% were added to mixtures with a chamber

volume fraction ( $\eta$ ) of 0.5 which is equivalent to an equivalence ratio ( $\Phi$ ) of 0.57. The effects of water vapor were studied by performing tests on mixtures containing a relative humidity of 0% and 100%.

#### 4.4.1 Effects of Water Vapor

Water vapor was found to have minimal influence on the peak pressure rise of mixtures containing HCFC-123. The peak pressure rise of mixtures containing 6.2% HCFC-123 decreased by 0.51 bar as the relative humidity was varied from 0% to 100%. Two factors may be responsible for this result:

1. The number of fluorine atoms is less in HCFC-123 when compared to HFC-125. The overall reaction rate is sensitive to water vapor when the F/H ratio is greater than unity. As the number of fluorine atoms is reduced the sensitivity of peak pressure rise with respect to water vapor decreases.
2. Even if the substitution of F atoms with Cl atoms does not have an effect on the sensitivity of a mixture to water vapor, unity between halogen atoms (X) and hydrogen atoms (H) exists at a HCFC-123 concentration of 7.5%. From the 2L experiments, the minimum inerting concentration was closer to, if not lower than, 7.5% which means a small window of flammable mixtures could contain an X/H ratio greater than unity. This range is dependent on the actual minimum inerting concentration, but the 2L results show it is less than 8.9% which is a significant improvement over the minimum inerting concentration of HFC-125, which was found to be 13.5% in the FAA aerosol can test. Mixtures containing HFC-125 at a concentration between 13.5% and 7.5% can be enhanced by the addition of water vapor while this can only happen for mixtures containing 8.9% to 7.5% HCFC-123, based on the results of the 2L tests.

#### **4.4.2 Effects of Nitrogen Dilution**

Nitrogen dilution was not examined for mixtures containing 8.9% and 11.2% HCFC-123 as the peak pressure rise was already well below the maximum allowable pressure rise illustrated by the black dotted line. With 21% oxygen in air, the mixture containing 6.2% HCFC-123 produced a peak pressure rise of 4.87 bar in the 2L chamber, which was above the threshold of 3.36 bar. When tests were performed on a similar mixture with 20% oxygen in air the peak pressure rise was reduced to 3.30 bar which was below the maximum allowable peak pressure rise by 1.7%. The results show that tests with nitrogen dilution resulting in 20% oxygen in air eliminates the overpressure for the mixtures tested with HCFC-123 as the suppressing agent. This is a solid result even though tests were not done at lower agent concentrations. From the FAA aerosol can test results, HFC-125 produced a consistent overpressure when added just below the sub inerting concentration (11.2%) and when added at quantities substantially lower the sub-inerting concentration (8.9% and 6.2%). 2-BTP was found to produce a larger overpressure when added at concentrations just below the sub-inerting concentration (5% and 6%) when compared to concentrations much lower than the sub-inerting concentration (3% and 4%). Based on the HFC-125 and 2-BTP results, it is predicted that HCFC-123 concentrations below 6.2% will not produce an overpressure in the FAA chamber if nitrogen dilution can reduce the amount of oxygen in air to 20%.

#### **4.5 HCFC-123 vs. HFC-125**

Tests results show the minimum inerting concentration of HCFC-123 to be lower than that of HFC-125. Mixtures containing HFC-125 at concentrations of 8.9% and 11.2% produced peak pressures in the 2L chamber that would have produced overpressures in the FAA chamber. Mixtures containing HCFC-123 at similar concentrations did not produce

any pressure rise in the 2L chamber. At 6.2% agent the maximum pressure rise was 7.07 bar for the mixture containing HFC-125 and 4.87 bar for the mixture containing HCFC-123. While the peak pressure rise of HCFC-123 was less than that of HFC-125 when added at 6.2%, an overpressure is still predicted. The reduction in peak pressure rise is likely due to the reduction in overall reaction rate predicted by the PSR calculations. As previously mentioned, the predicted peak pressure rise from constant volume equilibrium calculations was similar for the mixtures containing the two agents.

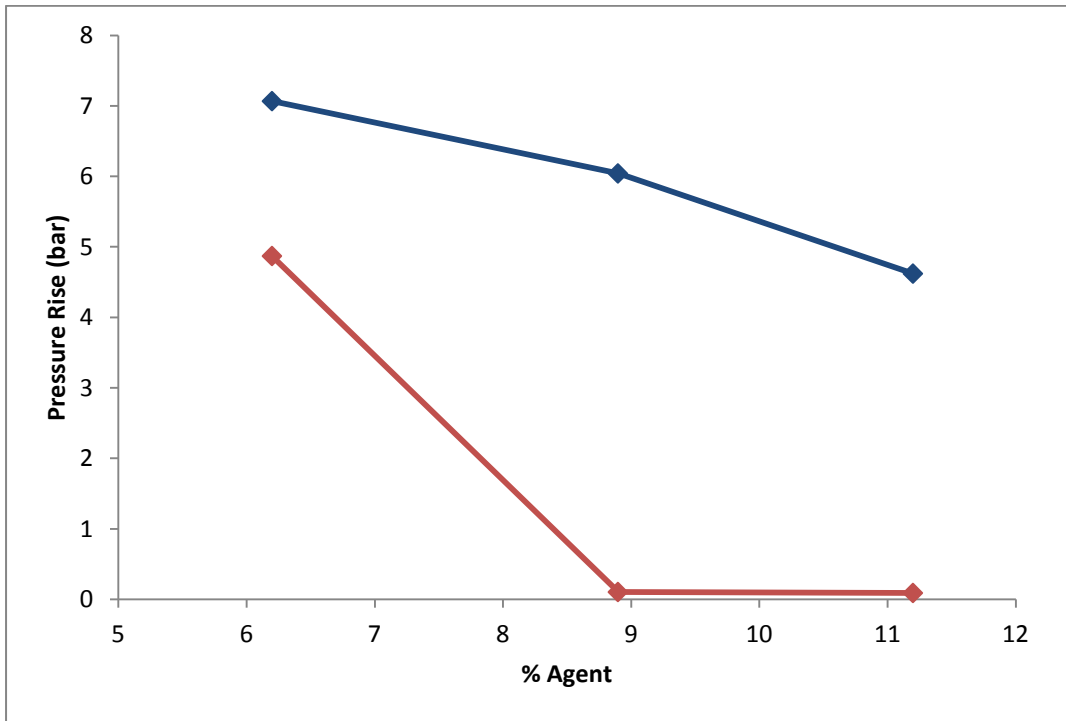


Figure 20: Peak pressure rise comparison of mixtures containing HFC-125 (blue) and HCFC-123 (red).

## 5. Conclusions

The following conclusions have been drawn from the computational and experimental work designed to increase the understanding of the FAA aerosol can test results.

1. When HFC-125 is added at sub-inerting concentrations to lean mixtures with an equivalence ratio below 0.6,  $\omega_{\text{psr}}$  increases. At an equivalence ratio of 0.4  $\omega_{\text{psr}}$  increases from  $16 \text{ s}^{-1}$ , with no agent, to  $685 \text{ s}^{-1}$  at an agent concentration of 6.25%. Generally, adding HCFC-123 to lean mixtures does not affect  $\omega_{\text{psr}}$  with the exception occurring at an equivalence ratio ( $\Phi$ ) of 0.4. The overall reaction rate ( $\omega_{\text{psr}}$ ) increases from  $16 \text{ s}^{-1}$  to  $31 \text{ s}^{-1}$  which is only 2.2% of the increase that occurs from adding HFC-125.
2. Water vapor was found to have a substantial influence on the peak pressure rise measured for mixtures containing ACTe fuel, air, and HFC-125. The increase in pressure rise resulting in added water vapor increased as the agent concentration increased. Increasing the agent concentrations results in a higher F/H ratio.
3. Nitrogen dilution resulting in 19% oxygen in air was tested for HFC-125 mixtures to determine if a dual HFC-125/nitrogen system could pass the aerosol can test. This level of dilution was not enough to reduce the pressure rise of mixtures containing 6.2% agent below the pressure rise estimated to cause an overpressure in the FAA chamber.
4. Computation and experimental results support the findings that adding HFC-125 at sub-inerting concentrations increases the pressure rise of lean mixtures. The results also support the previously estimated values of chamber volume mixing that took place in during tests with HFC-125 in the FAA aerosol can test.

5. HCFC-123 was found to have a lower minimum inerting concentration than HFC-125. The actual value was not determined but tests showed that 8.9% HCFC-123 was capable of suppressing the 2L chamber reaction.
6. HCFC-123 was found to be less sensitive to the presence of water vapor as the minimum inerting concentration is closer to the concentration where X/H is unity (X being the amount of halogen atoms and H being the amount of hydrogen atoms).
7. The pressure rise of mixtures containing HCFC-123 was lower than similar mixtures containing HFC-125. This shows that the kinetics are indeed slower than mixtures containing HFC-125 but not slow enough to reduce the pressure rise below the level that would cause overpressures.
8. Nitrogen dilution was studied on HCFC-123 mixtures and it was found that adding nitrogen resulting in 20% oxygen in air successfully reduced the peak pressure rise (3.30 bar) below the level that would cause overpressures (3.36 bar).

## 5.1 Future Work

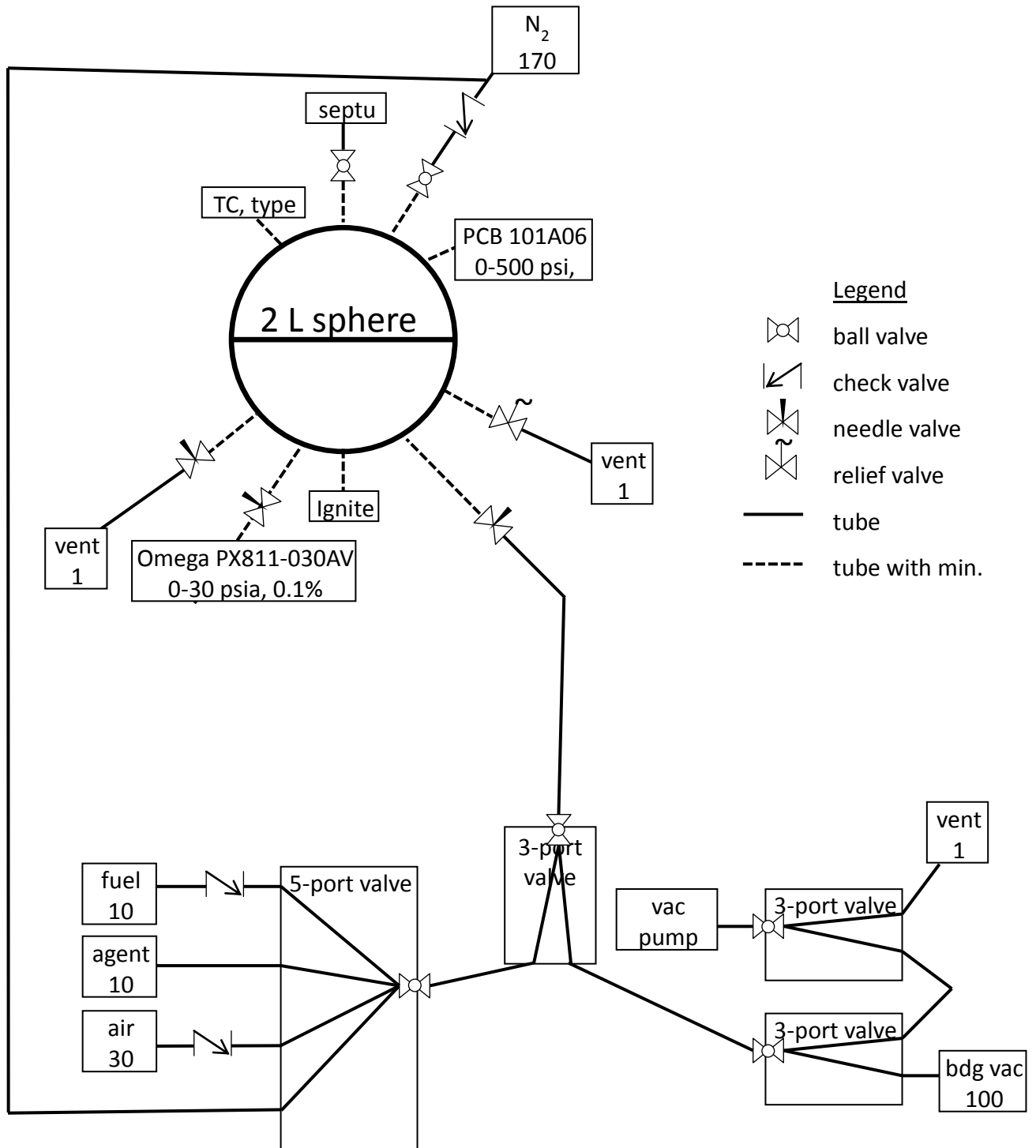
Useful information was obtained from the experimental analysis which suggested the need for continued work. The following tasks could be performed to solidify the conclusions drawn from this report:

1. Continue work to estimate the required amount of nitrogen dilution that will stop HFC-125 from causing overpressures in the FAA chamber.
2. Determine the minimum inerting concentration of HCFC-123 in the 2L chamber for mixtures containing ACTe fuel, air, and agent.
3. Perform tests at lower concentrations of HCFC-123 to ensure overpressures will not occur with nitrogen dilution resulting in 20% oxygen in air.
4. Measure the burning velocity of mixtures to provide data for kinetic mechanism validation.

# Appendices

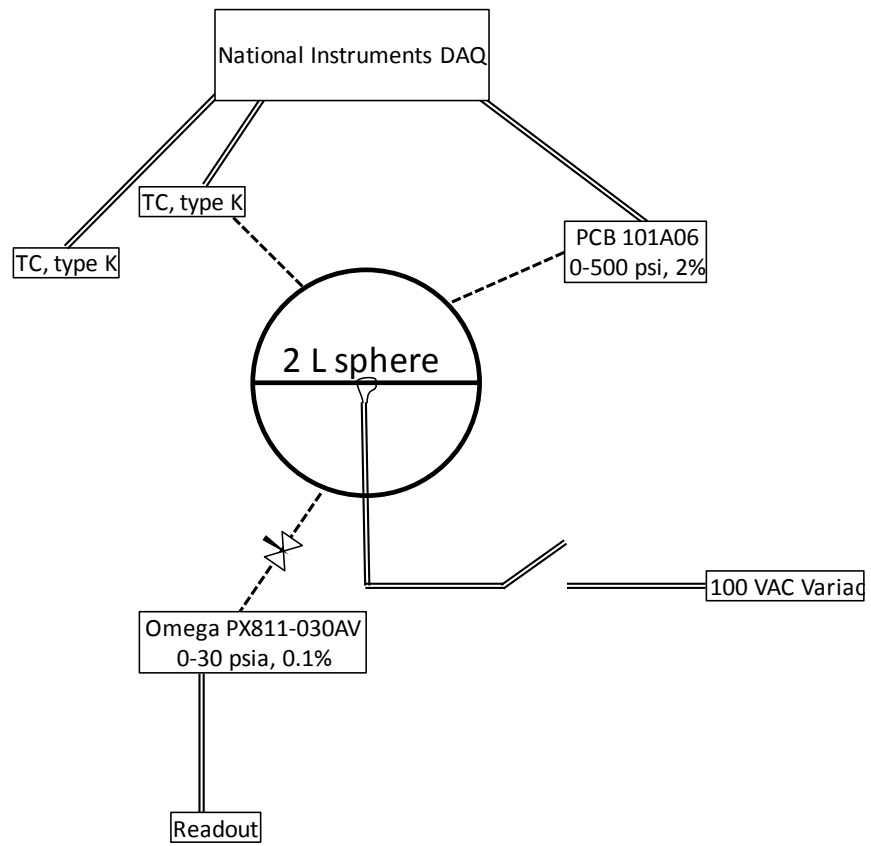
## 1. 2L Chamber Schematics

### Plumbing Schematic





## Electrical Schematic



## 2. Pressure Vessel Safety Considerations

Stress calculations were performed on the 2 L chamber design to determine the maximum allowable pressure rise. Spherical pressure vessel standards were found in the ASME Boiler and Pressure Vessel Code, Section VIII. Code UG-27 (d) for calculating the thickness of spherical shells under internal pressure was used to show the two hemispherical shells were capable of withstanding over 2500 bar. Appendix 2-4 (2) for calculating the stress on internal type flanges was utilized to show that the flange and bolts could withstand 400 bar. Calculations are presented in Table 1 and Table 2. All valves connected to the chamber were rated for at least 344 bar. The polymer o-ring that seals the two hemispheres was found to be the constraining element with a maximum operating pressure of 100 bar.

The UG-99 standard hydrostatic test was conducted as an extra safety precaution to ensure the chamber could safely operated in the estimated peak pressure range of anticipated experiments. Pressure testing a vessel with a liquid such as water is safer as the compressibility is much less than a gas. If any part of the chamber were to burst the water would just trickle out unlike a compressed gas that would expand rapidly. Pressure testing with water also makes it easier to find small leaks as the water is evident on the exterior. Hydrostatic tests were performed without the pressure relief valve installed up to 40 bar without any signs of deformation or leakage. Equilibrium calculations were performed for various mixtures at atmospheric conditions to show a maximum final pressure of around 11 bar, which is well below the 40 bar for which the chamber was pressure tested.

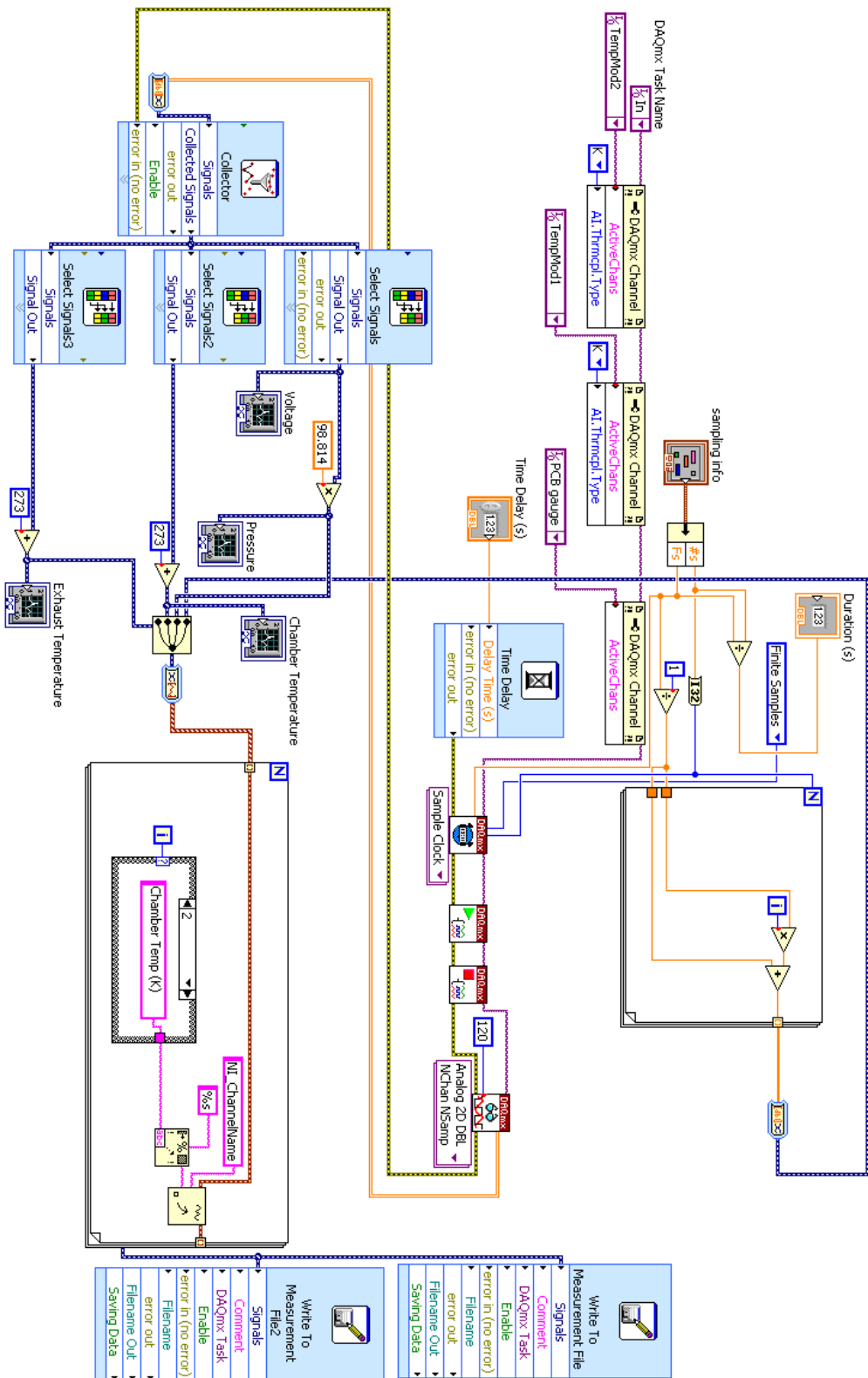
**Table 1: Integral Flame Calculation.**

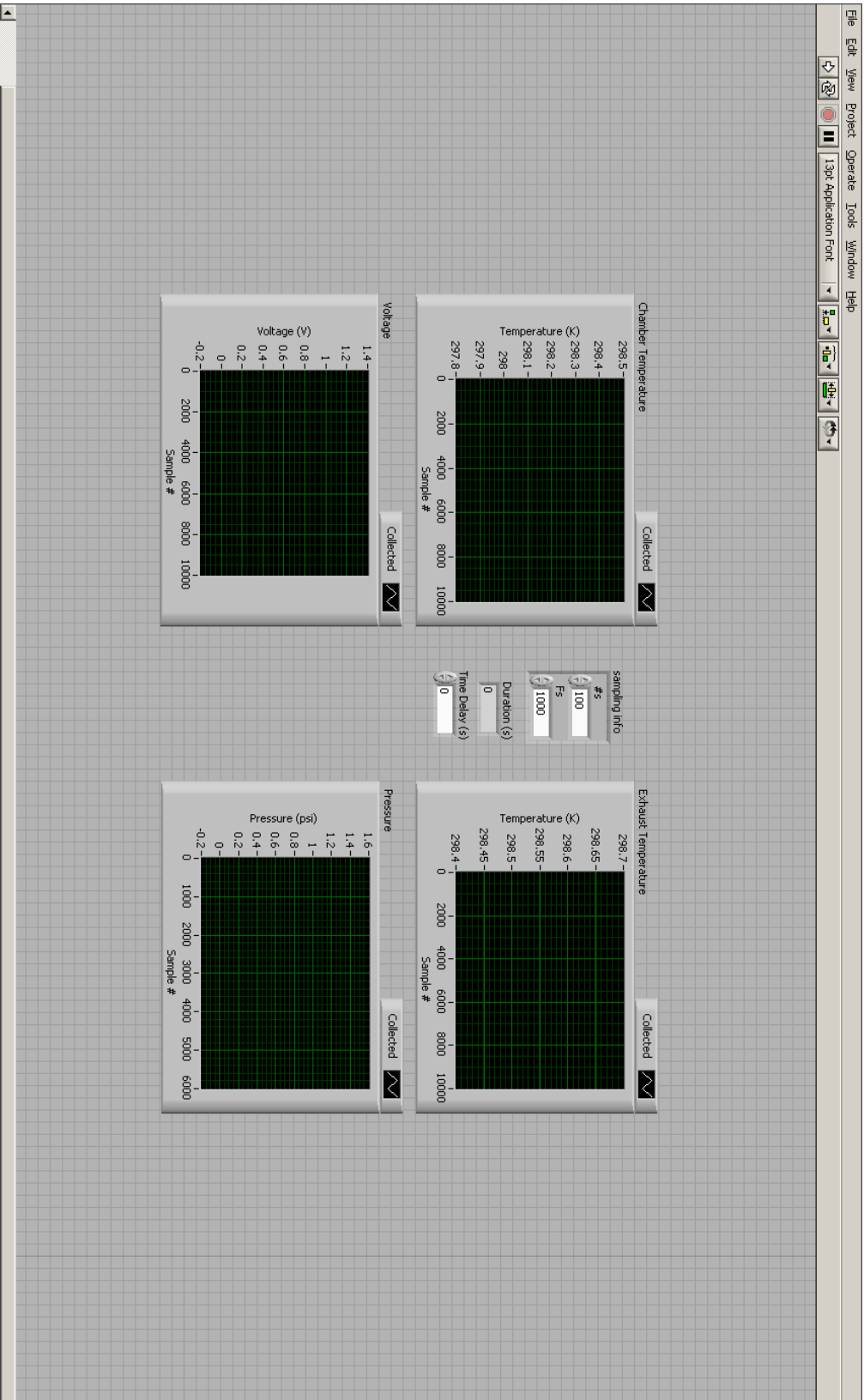
Integral Flange - Reactor Shell - Low Temperature				Items in blue must be entered			
From The ASME Boiler and Pressure Vessel Code, Section VIII, Division 1, Appendix							
Bolt load for gasket seating ( $W_{m2}$ ) assumes a selfenergizing o-ring with no seating lo							
Design Conditions		Gasket Details		Flange Dimensions			
Design Pressure	6000	G (dia.)=	6.725	t (thickness)=	1.00	$g_1$ =	1.00
Design Temperature	70	b=	0.105	A (O.D.)=	10.25	R=	0.63
Flange Material	316 SS	N=	0.21	B (I.D.)=	6.00	h=	2.00
Bolting Material	Metal Alloy	y=	0	C (bolt circle)=	9.25	$g_0$ =	1.00
Corrosion Allowance	0	m=	0				
Allowable Stress		Load and Bolt Calculations					
Flange	Design Temp	74690	Size=	"3/8-16"	$W_{m2}$ =	0	$A_m$ = (greater of) 0.000 or 1.33 using 1.33
	Atm. Temp, S	74690	No. bolts=	8	$H_p$ =	0	$A_b$ (act.)= 0.53
Bolt	Design Temp	160000	Root dia.=	0.29	H=	213013	W= 148758
	Atm. Temp, S	160000			$W_{m1}$ =	213013	
Condition	Load	Lever Arm	Moment	Stress Calculation-Operating		Allowable Stress	
Operating	$H_D$ = 169560	$h_D$ = 1.125	$M_D$ = 190755	Long. Hub, $S_H$ =	46972	1.5 $S_{fo}$	112035
	$H_G$ = 0	$h_G$ = 1.2625	$M_G$ = 0	Radial Flg., $S_R$ =	70182	$S_{fo}$	74690
	$H_T$ = 43453	$h_T$ = 1.44375	$M_T$ = 62735	Tang. Flg., $S_T$ =	17163	$S_{fo}$	74690
			$M_0$ = 253490	greater of .5(SH+SR)	58577	$S_{fo}$	74690
Seating	$H_G=W$ = 148758	$h_G$ = 1.2625	$M_G$ = 187807	or .5(SH+ST)	32068	$S_{fo}$	74690
K and Hub Factors (some from graphs)			Stress Formula Factors	Stress Calculation-Seating		Allowable Stress	
K= 1.71	$h/h_0$ = 0.82		t= 1.00	Long. Hub, $S_H$ =	34801	1.5 $S_{fo}$	112035
T= 1.62	$F$ = 0.91	From Fig. 2-7.2	alpha= 1.37	Radial Flg., $S_R$ =	51997	$S_{fo}$	74690
U= 4.17	$V$ = 0.55	From Fig. 2-7.3	beta= 1.49	Tang. Flg., $S_T$ =	12716	$S_{fo}$	74690
Y= 3.80	$f$ = 1	From Fig. 2-7.6	gamma= 0.85	greater of .5(SH+SR)	43399	$S_{fo}$	74690
Z= 2.04	e= 0.37		delta= 0.05	or .5(SH+ST)	23758	$S_{fo}$	74690
$g_1/g_0$ = 1.00	d= 18.59		epsilon= 0.90				
$h_0$ = 2.45			$m_0$ = 42248				
			$m_G$ = 31301				

**Table 2: Hemispherical Head Calculation.**

Hemispherical Head Calculation	
Equations taken from ASME Section VIII-1, UG-27	
<b>316 SS Sphere Properties</b>	
Max tensile stress, S (psi)	74694
Inner Radius, L (in)	3
thickness, t (in)	1
Lowest Efficiency, E	0.8
<b>For thin walled equations to be valid</b>	
t must be less than (in)	1.068
P must be less than (psi)	39737
<b>Max Allowable Pressure (psi)</b>	<b>37347</b>

### 3. LabView VI Block Diagram and Front Panel





## 4. Complete List of Procedures

### Operating Procedure:

1. Verify desired initial conditions of test:
  - pressure
  - temperature
  - composition (fuel, air, humidity)
  - ignition type (wire or spark)
  - sensor type (dP/dt, T, or both)
  - locate and get ready to fill in lab notebook book.
2. Verify that vent is working (Magnehelic gage at 0.2 in. water, vent sucking air, exhaust fans audible).
3. Verify igniter power off.
4. Turn N<sub>2</sub>, reactant air, and reactant fuel, and reactant agent bottles on.
5. Pressure purge chamber (see below).
6. Pressure test chamber and pressure relief valve (see below).
7. Vacuum vent chamber (see below).
8. Install Platinum igniter (see below).
9. Vacuum test chamber (see below).
10. Vacuum vent chamber (see below).
11. Use the vacuum pump to draw a vacuum below 1 Torr.
12. Add liquids reactants (if applicable) in order from lowest to highest vapor pressure. If there are no liquid reactants skip to step 14.
  - a. Use syringe to obtain the desired volume of liquid.
  - b. Determine the mass of the liquid using the Mettler PE 360 scale.
  - c. Record mass and volume into lab notebook.
  - d. Remove septum cover and inject liquid into chamber.
  - e. Record the pressure at 1 min increments for 10 min or until the pressure increases less than 0.02 Torr/min.
13. Repeat step 12 for each liquid reactant.
14. Add air to chamber:
  - a. Set 5-way valve to air.
  - b. Set secondary chamber fill valve to 5-way.
  - c. Using the main chamber fill valve to establish the desired air pressure
  - d. Record pressure at 1 min increments for 5 min, then record final fill pressure.
15. Purge fill lines with fuel (propane).
  - a. Select propane with fuel selection valve.
  - b. Set 5-way valve to fuel.
  - c. Switch secondary chamber fill valve back and forth between chamber vac and 5-way valve 5 times while waiting 10 s each time when the valve is set to chamber vac.
  - d. End purge with secondary chamber valve facing 5-way valve.
16. Add fuel (propane) to chamber:
  - a. Open the main chamber valve; establish the desired pressure in chamber.
  - b. Record pressure at 1 min increments for 5 min, then record final fill pressure.

- c. Verify main chamber fill valve is closed.
17. Purge fill lines with agent (CF<sub>3</sub>BR, R125, or Novec 1230).
  - a. Set 5-way valve to refrigerant.
  - b. Switch secondary chamber fill valve back and forth between chamber vac and 5-way valve 5 times while waiting 10 s each time when the valve is set to chamber vac.
  - c. End purge with secondary chamber valve facing 5-way valve.
18. Add agent (CF<sub>3</sub>BR, R125, or Novec 1230) to chamber:
  - a. Open the main chamber valve; establish the desired pressure in chamber.
  - b. Record pressure at 1 min increments for 5 min, then record final fill pressure.
  - c. Verify main chamber fill valve is closed.
19. Wait 15 min to allow reactants to mix and settle.
20. Close Omega pressure sensor valve.
21. Close septum valve.
22. Plug ignitor into Variac.
23. Verify N<sub>2</sub> inlet valve, Omega pressure gage valve, purge vent valve, main chamber fill valve, septum valve, all closed.
24. Verify thermocouples working.
25. Verify PCB pressure gage working.
26. Start Labview vi.
27. Flip the Variac ignition switch manually for 2 s and then switch it off.
28. Unplug ignitor plug from Variac.
29. Open the N<sub>2</sub> inlet valve.
30. Open the Purge vent valve.
31. Wait 1 min.
32. Close N<sub>2</sub> inlet valve.
33. Close Purge vent valve.
34. Test Variac with lamp.
35. Pressure purge chamber (see below).
36. Vacuum vent chamber (see below).
37. Pressure purge chamber (see below).
38. Vacuum vent chamber (see below).
39. Verify data is collected.
40. Shut down DAS.
41. Shut all gas valves on supply gases.

### **Pressure Purge Chamber:**

1. Verify all chamber valves closed.
2. Open the Air inlet valve.
3. Open purge vent valve.
4. Purge for 2 min.
5. Close air inlet valve.
6. Close purge vent valve.

### **Pressure Test Chamber and Pressure Release Valve:**

1. Verify all valves closed.
2. Set N<sub>2</sub> regulator to 170 psig (nominal).
3. Open N<sub>2</sub> inlet valve.
4. Verify the pressure relief valve opens.
5. Close N<sub>2</sub> inlet valve.
6. Set regulator to 160 psig (nominal).
7. Open N<sub>2</sub> inlet valve.
8. Wait 2 min and verify that the chamber pressure has not decreased by more than 2 psig.
9. Close N<sub>2</sub> inlet valve.
10. Open the purge vent valve and vent chamber to ambient.
11. Close all valves.

### **Vacuum Vent Chamber:**

1. Verify chamber pressure is at ambient or lower
2. Open Omega pressure gage valve.
3. Verify purge vent valve closed
4. Set secondary chamber fill valve to chamber vac.
5. Open main chamber fill valve.
6. Wait for the chamber to reach approximately 100 Torr on Omega readout.
7. Maintain vacuum for 5 min.
8. Close main chamber fill valve.
9. Set 5-way valve to air
10. Set secondary fill valve to 5-way
11. Open main chamber fill valve and slowly bring pressure to ambient.
12. Close main chamber fill valve.
13. Close secondary chamber fill valve.

### **Vacuum Test Chamber:**

1. Verify chamber pressure is at ambient or lower.
2. Open the Omega pressure gage valve.
3. Set the secondary chamber fill valve to chamber vac.
4. Open main chamber fill valve.
5. Wait for the chamber to reach approximately 100 Torr.
6. Close the main chamber fill valve and wait 2 min. Verify that chamber pressure has not increased by more than 0.2 Torr.
7. Set 5-way valve to air
8. Set secondary fill valve to 5-way
9. Open main chamber fill valve and slowly bring pressure to ambient.
10. Close main chamber fill valve.
11. Close secondary chamber fill valve.



### **Platinum Igniter Installation:**

1. Verify chamber at ambient laboratory pressure (open purge vent valve, and close.).
2. Verify igniter power off.
3. Remove igniter plug from Variac outlet.
4. Put on Nitrile gloves.
5. Remove igniter assembly.
6. Remove old igniter Platinum wire from assembly and discard.
7. Install new Platinum wire in assembly.
8. Install igniter assembly.
9. Discard Nitrile gloves.
10. Test resistance across igniter leads at plug, and record.
11. Check for resistance  $> 1000 \Omega$  from either lead of igniter to chamber body.

### **Procedure for Removing Chamber Wall Soot:**

1. Vacuum vent chamber with vacuum pump for one hour.
2. Open the Omega pressure gage valve.
3. Set 5-way valve to air.
4. Set secondary chamber valve to 5-way valve.
5. Open main chamber fill valve and raise the pressure in the chamber to 800 Torr.
6. Open purge vent valve to bring the chamber to ambient pressure.
7. Close all valves.
8. Disconnect PCB pressure gage cable, chamber thermocouple, and Nitrogen line from the upper half of the chamber.
9. Use torque wrench to remove connector bolts.
10. Place cardboard near chamber.
11. Remove upper half of chamber and place on cardboard.
12. Put on Nitrile gloves.
13. Clean inner chamber walls and threaded ports using kim-wipes and bulk ethanol.
14. Use shop-vac to remove any pieces of kim-wipe left in chamber.
15. Put upper chamber half back in place and reconnect with bolts.
16. Reconnect PCB pressure gage cable, chamber thermocouple, and Nitrogen line to upper chamber half.
17. Vacuum vent chamber.

### **Safety Considerations:**

42. When removing igniter, be sure igniter is un-plugged and Variac is powered down.
43. Wear ear muffs when igniting the combustible mixture.

44. In the event of a power failure, water leak in the lab, emergency evacuation, etc., shut off all valves and leave the room.
45. The chamber is heavy and is a lifting/dropping hazard. For lifting, use two people when appropriate. Routine operation of the 2 L chamber does not require removal of the top half. When it does, remove the top fitting (1/2" NPT) and insert the lifting handle to make handling easier, and wear leather gloves.
46. If a supply line fails during the fill procedure, shut off the gas supply to that line.

**Emergency Shutdown:**

1. Each experimental run test time is less than a second, and after an experiment run, there are no hazards associated with this tool operating unattended; therefore, the instrument itself it does not need to be shutdown in an emergency (see #2 below).
2. In an event the tool must be shut down immediately, shut all gas-supply valves and turn off igniter power supply.
3. If an alarm occurs for fire, shelter in place, etc., shut off gases at the supply bottle and immediately leave the room. It is not necessary to shutdown the instrument.
4. If the emergency is in the lab, leave immediately and contact NIST emergency operator at extension x2222.

## 5. Summary of FAA Test Results with Mixture Conversion to 2L Chamber [Sunderland]

LJW, Reinhardt, Behavior of Bromotrifluoropropane..., FAA, May, 2004														
TABLE 1. SUMMARY OF TEST RESULTS														
Corrected entries from Table 1-->														
Test Number	Test ID	Date	Agent	FREX Type	Charge Weight (lbs)	Charge Pressure (psig)	Discharge Time (min)	Discharge Weight (lbs)	Agent Peak Concentration (%)	Air Temperature (Deg F)	Fire Event	Peak Temp (Deg F)	Peak Pressure (psig)	Comments
1	N/A	24-Nov-03	None	386 LRD	8.5	150	28.5	5*	2.5	72	N/A	N/A	N/A	FAA Analyzer to Statham comparison/No FAA computer data available
2	112503T1	25-Nov-03	BTP	386 LRD	10.6*	260	29.7	5*	2.5	67	Yes	368	>64 psia	Transducer saturated at 60 psia
3	120203T1	2-Dec-03	None	386 LRD	N/A	N/A	N/A	N/A	0	65	Yes	397	25.4	No BTP used in test - Baseline
4	120203T2	2-Dec-03	None	386 LRD	N/A	N/A	N/A	N/A	0	68	Yes	328	23.4	No BTP used in test - Baseline
5	120203T3	2-Dec-03	BTP	386 LRD	12.4*	262	27.1	5.5*	3	70	Yes	1056	63	
6	120903T1	3-Dec-03	BTP	386 LRD	11*	272	40.8	6.9*	4	65	Yes	1095	63	
7-abort	120403T1	4-Dec-03	BTP	386 LRD	12.5*	360	71	11.4*	6	59	No	N/A	N/A	Location of igniter shield low, arc suppress by liquid
8	120403T2	4-Dec-03	BTP	386 LRD	10.5	360	40.4	10.5*	5	50	No	N/A	N/A	High agent usage - test setup eval.
9	120803T1	8-Dec-03	BTP	386 LRD	12	360	43.3	9.75	5	66	Yes	1251	100	Calculated agent weight is 8.5 lbs -1.25 lb discrepancy
10	120903T1	9-Dec-03	BTP	386 LRD	12.5	360	50.6	11.9	6	53	N/A	N/A	N/A	Questionable readout on simulator transducer. No test. Short on transducer signal.
11-abort	121003T1	10-Dec-03	BTP	386 LRD	12.5	362	48.3	11.1	6	63	N/A	N/A	N/A	No test, igniter failed to work. Test aborted
12-abort	121003T1B	10-Dec-03	BTP	386 LRD	12.5	362	45.5	11.1	6	62	Partial	78	0	Small flame near ceiling area. Fan left on. Igniter 2 inches below ramp. Alcohol residue burning on igniters (small flames).
13	121103T1	11-Dec-03	BTP	386 LRD	12.5	362	46.5	11.1	6	63	Yes	1467	93	
14	121503T1	15-Dec-03	BTP	386 LRD	13	360	55.5	11.1	6	62	N/A	N/A	N/A	Heat gun test - no effect on the decomposition of BTP after 30 minutes activation
15	121503T1	15-Dec-03	BTP	386 LRD	1.9	360	55.5	11.1	5	62	N/A	N/A	N/A	Heat gun test - no effect on the decomposition of BTP after 10 minutes activation
16	121603T1	16-Dec-03	Halon 1301	386 LRD	9	360	16 sec.	3.63	2.5	53.2	Yes	65	4	Halon 1301 used during this test
17	010704T1	7-Jan-04	HFC-125	HRD	11.2	360	<1 min	Not Recorded	8.9	Yes	1227	53		HFC125
18-abort	010804T1	8-Jan-04	HFC-125	HRD	17.5	360	<1 min	Not Recorded	11	N/A	N/A	N/A	N/A	HFC125, igniter arc malfunctioned and suppressed by simulator liquid
19	010904T1	9-Jan-04	HFC-125	HRD	17	360	<1 min	Not Recorded	11	Yes	1067	52		HFC125
20	011304T1a	13-Jan-04	HFC-125	HRD	30	360	<1 min	Not Recorded	13.5	49.6	No	N/A	N/A	HCF-125. Air added to drop concentration to required concentration; redundant igniter used
21-high p	011304T1b	13-Jan-04	HFC-125	HRD	30	360	<1 min	Not Recorded	6.3	49.6	No	N/A	N/A	HFC-125. Pressure chamber pressurized to 20 psig and electrodes arcing. No simulator activation.
22-high p	011304T2a	13-Jan-04	HFC-125	HRD	30	360	<1 min	Not Recorded	6.1	50	No	N/A	N/A	HFC-125. Pressure chamber pressurized to 20 psig and electrodes arcing. No simulator activation.
23	011304T2b	13-Jan-04	HFC-125	HRD	30	360	<1 min	Not Recorded	6.2	50	Yes	1026	52	HFC-125. Pressure vessel at ambient pressure
														HFC-125. Pressure vessel pressurized to 15 psig. Igniter was activated, but no event (simulator not used).
24-high p	011404T1a	14-Jan-04	HFC-125	HRD	30	360	<1 min	Not Recorded	11.3	24	No	N/A	N/A	HFC-125. Pressure vessel pressurized to 15 psig. Simulator activated.
25-high p	011404T1b	14-Jan-04	HFC-125	HRD	30	360	<1 min	Not Recorded	11.3	24	Yes	32	6	

\* Estimated as a result of scale used during test.

HRD= High Rate Discharge

LRD= Low Rate Discharge

Outdoor conds-->										FAA chamber conds-->										moles denat ethanol= 5.907 Assuming eta=1-->										For specified eta-->									
										chamber L= 11383										moles H2O from aerosol= 5.036																			
avg outdoor T, F	avg outdoor RH	avg outdoor p, in	avg outdoor T, C	avg outdoor pH2O, Torr	avg outdoor XH2O	test p, psig	Air T, C	moles/L	moles dry air	moles agent	moles H2O	X dry air	X agent	X H2O	X ethanol	X propane	check sum	eta	moles dry air	moles agent	moles H2O																		
57.1867	0.882	29.98133	13.99259	10.520429	0.013871	0	22.222	0.0413	452.48798	11.7554495	11.4	0.9356	0.0243	0.0236	0.0122	0.00425	1	0.5	226.2	5.8827	8.21792																		
42.19	0.517	30.153	5.661111	3.5181077	0.004655	0	19.444	0.042	453.6877	11.9451521	7.209	0.9447	0.0243	0.0147	0.012	0.00419	1	0.5	231.8	5.9726	6.12226																		
37.77	0.418	30.216	3.205556	2.3925553	0.003179	0	18.333	0.0422	479.1015	0	6.554	0.9706	0	0.0133	0.012	0.00417	1	0.3	143.7	0	5.49406																		
37.77	0.418	30.216	3.205556	2.3925553	0.003179	0	20	0.042	476.37753	0	6.555	0.9704	0	0.0134	0.012	0.00419	1	0.3	142.9	0	5.49145																		
37.77	0.418	30.216	3.205556	2.3925553	0.003179	0	21.111	0.0418	460.34149	14.2827745	6.504	0.9412	0.0292	0.0133	0.0121	0.00421	1	0.5	230.2	7.1414	5.75975																		
30.82	0.426	30.536	-0.65556	1.8441576	0.002476	0	18.333	0.0427	465.13611	19.4287847	6.19	0.9327	0.039	0.0124	0.018	0.00412	1	0.5	232.6	9.7144	5.613																		
36.07	0.495	30.453	2.261111	2.6485123	0.003547	0	15	0.043	458.98907	29.4001762	6.689	0.9125	0.0584	0.0133	0.0117	0.00409	1	0.5	229.5	14.7	5.85248																		
36.07	0.495	30.453	2.261111	2.6485123	0.003547	0	10	0.0438	472.04264	24.9327823	6.716	0.9226	0.0487	0.0131	0.0115	0.00402	1	0.5	236	12.466	5.87575																		
31.22	0.618	30.146	-0.43333	2.7193689	0.003605	0	18.889	0.042	453.03459	23.9301949	6.675	0.9215	0.0487	0.0136	0.012	0.00418	1	0.5	226.5	11.965	5.8552																		
37.23	0.67	30.27	2.905556	3.7540041	0.00497	0	11.667	0.0433	460.8785	29.5655182	7.35	0.9113	0.0585	0.0145	0.0117	0.00407	1	0.5	230.4	14.783	6.19295																		
48.03	0.928	30.07	8.905556	7.8936663	0.010438	0	17.222	0.0422	446.61817	28.8082471	9.747	0.9057	0.0584	0.0198	0.012	0.00417	1	0.5	223.3	14.404	7.39116																		
48.03	0.928	30.07	8.905556	7.8936663	0.010438	0	16.667	0.0423	447.47431	28.8634703	9.756	0.9057	0.0584	0.0197	0.012	0.00416	1	0.5	223.7	14.432	7.39567																		
55.0158	0.926842105	29.25	12.78655	10.21663	0.013141	0	17.222	0.041	433.2522	28.0226548	10.81	0.9025	0.0584	0.0225	0.0123	0.00429	1	0.5	216.6	14.011	7.92033																		
39.2182	0.676363636	29.84727	4.010101	4.0988879	0.00538	0	16.667	0.0419	446.4302	28.6496797	7.45	0.9102	0.0584	0.0152	0.012	0.00419	1	0.5	223.2	14.325	6.24303																		
39.2182	0.676363636	29.84727	4.010101	4.0988879	0.00538	0	16.667	0.0419	451.17946	23.8747331	7.476	0.9198	0.0487	0.0152	0.012	0.00419	1	0.5	225.6	11.937	6.25587																		
41.89	0.735	30.198	5.494444	4.9437498	0.006565	0	11.778	0.0432	475.96456	12.2848716	8.181	0.9436	0.0244	0.0162	0.0117	0.00408	1	0.5	238	6.1424	6.60836																		
24.53	0.363	30.267	-4.15	1.2105363	0.001611	0	-17.778	0.0483	499.80548	48.9072171	5.842	0.8885	0.0889	0.0104	0.0105	0.00366	1	0.5	249.9	24.454	5.43894																		
29.25	0.431	30.305	-1.52778	1.7494489	0.002331	0	-17.778	0.0483	488.54452	60.5230132	6.177	0.8674	0.1075	0.011	0.0105	0.00365	1	0.5	244.3	30.262	5.60648																		
26.58	0.474	30.25	-3.01111	1.7224982	0.002291	0	-17.778	0.0482	487.67746	60.4131711	6.156	0.8674	0.1075	0.0109	0.0105	0.00366	1	0.5	243.8	30.207	5.59565																		
43.1	0.618	29.894	6.168667	4.3559284	0.005726	0	9.7778	0.043	421.32548	66.1347071	7.462	0.8378	0.1315	0.0148	0.0117	0.00409	1	0.5	210.7	33.067	6.24891																		
43.1	0.618	29.894	6.168667	4.3559284	0.005726	20	9.7778	0.1016	1077.5104	72.8645625	11.24	0.9213	0.0623	0.0096	0.0051	0.00176	1	0.5	538.8	36.432	8.13849																		
43.1	0.618	29.894	6.168667	4.3559284	0.005726	20	10	0.1015	1078.9629	70.4860509	11.25	0.9232	0.0603	0.0096	0.0051	0.00176	1	0.5	539.5	35.248	8.14267																		
43.1	0.618	29.92	6.168667	4.3559284	0.005731	0	10	0.043	456.91862	30.3755551	7.669	0.9085	0.0604	0.0152	0.0117	0.00409	1	0.5	228.5	15.188	6.35256																		
20.38	0.417	30.157	-6.45556	1.1655545	0.001546	15	-4.4444	0.0924	931.21364	118.816286	6.477	0.8748	0.1116	0.0061	0.0055	0.00193	1	0.5	465.6	59.408	5.75645																		
20.38	0.417	30.157	-6.45556	1.1655545	0.001546	15	-4.4444	0.0924	931.21364	118.816286	6.477	0.8748	0.1116	0.0061	0.0055	0.00193	1	0.5	465.6	59.408	5.75645																		

FAA chamber conds-->		1.85 L chamber conds-->		chamber L= 1.85		1.85 L chamber conds-->		chamber L= 1.85		1.85 L chamber conds-->		chamber L= 1.85						
X dry air	X agent	X H2O	X ethanol	X propane	check sum	P, Torr	T, C	mole%L	g H2O	rho H2O, g/m3	usat H2O, Torr	RH H2O	rho ethanol, g/m3	cc ethanol	usat ethanol, Torr	RH ethanol		
0.91114	0.02369	0.0331	0.02379	0.00828	1	761.6	23	0.04124	0.04548	998	0.0456	21	1.2	0.08361	787.75	0.1061	52.2666	0.3466
0.92037	0.02371	0.0243	0.02345	0.00817	1	765.9	23	0.04147	0.03359	998	0.0337	21	0.89	0.08289	787.75	0.1052	52.2666	0.3437
0.91438	0	0.03495	0.03758	0.01309	1	767.5	23	0.04156	0.04841	998	0.0485	21	1.28	0.13312	787.75	0.169	52.2666	0.5519
0.91395	0	0.03612	0.03778	0.01316	1	767.5	23	0.04156	0.04864	998	0.0488	21	1.28	0.13382	787.75	0.1699	52.2666	0.5548
0.91685	0.02845	0.02298	0.02363	0.00819	1	767.5	23	0.04156	0.03183	998	0.0319	21	0.84	0.08336	787.75	0.1058	52.2666	0.3455
0.90897	0.03797	0.02194	0.02309	0.00804	1	775.6	23	0.042	0.03071	998	0.0308	21	0.81	0.08266	787.75	0.1049	52.2666	0.3426
0.88947	0.06698	0.02268	0.0229	0.00797	1	773.5	23	0.04189	0.03167	998	0.0317	21	0.84	0.08174	787.75	0.1038	52.2666	0.3389
0.89972	0.04752	0.0224	0.02252	0.00784	1	773.5	23	0.04189	0.03127	998	0.0313	21	0.82	0.08039	787.75	0.1021	52.2666	0.3333
0.8978	0.04742	0.02321	0.02341	0.00815	1	765.7	23	0.04146	0.03207	998	0.0321	21	0.85	0.08274	787.75	0.105	52.2666	0.343
0.88843	0.06699	0.02388	0.02278	0.00793	1	768.9	23	0.04163	0.03313	998	0.0332	21	0.87	0.08082	787.75	0.1026	52.2666	0.335
0.8824	0.06692	0.02921	0.02334	0.00813	1	763.8	23	0.04136	0.04026	998	0.0404	21	1.06	0.08228	787.75	0.1045	52.2666	0.3411
0.88249	0.06692	0.02917	0.0233	0.00811	1	763.8	23	0.04136	0.04021	998	0.0403	21	1.06	0.08213	787.75	0.1043	52.2666	0.3405
0.87873	0.06684	0.03213	0.02396	0.00834	1	743.0	23	0.04023	0.04308	998	0.0432	21	1.14	0.08217	787.75	0.1043	52.2666	0.3406
0.88666	0.0669	0.0248	0.02347	0.00817	1	758.2	23	0.04105	0.03393	998	0.034	21	0.9	0.0821	787.75	0.1042	52.2666	0.3404
0.8961	0.04742	0.02465	0.02347	0.00817	1	758.2	23	0.04105	0.034	998	0.0341	21	0.9	0.0821	787.75	0.1042	52.2666	0.3404
0.91992	0.02374	0.02554	0.02284	0.00795	1	767.1	23	0.04153	0.03536	998	0.0354	21	0.93	0.08084	787.75	0.1026	52.2666	0.3351
0.88844	0.08498	0.0189	0.02053	0.00715	1	768.8	23	0.04163	0.02622	998	0.0263	21	0.69	0.07284	787.75	0.0925	52.2666	0.302
0.84786	0.10504	0.01946	0.0205	0.00714	1	769.8	23	0.04168	0.02703	998	0.0271	21	0.71	0.07284	787.75	0.0925	52.2666	0.302
0.84782	0.10503	0.01946	0.02054	0.00715	1	768.4	23	0.04161	0.02698	998	0.027	21	0.71	0.07284	787.75	0.0925	52.2666	0.302
0.8167	0.1282	0.02423	0.0229	0.00798	1	759.3	23	0.04112	0.0332	998	0.0333	21	0.88	0.08026	787.75	0.1019	52.2666	0.3327
0.91115	0.06161	0.01376	0.00999	0.00348	1	1793.6	23	0.09712	0.04455	998	0.0447	21	1.18	0.0827	787.75	0.105	52.2666	0.3429
0.91308	0.06966	0.01378	0.01	0.00348	1	1793.6	23	0.09712	0.04461	998	0.0447	21	1.18	0.08276	787.75	0.1051	52.2666	0.3431
0.88562	0.06888	0.02463	0.0229	0.00797	1	760.0	23	0.04115	0.03377	998	0.0339	21	0.89	0.08032	787.75	0.102	52.2666	0.333
0.86426	0.11027	0.01069	0.01097	0.00382	1	1541.7	23	0.08348	0.02973	998	0.0298	21	0.78	0.07802	787.75	0.099	52.2666	0.3235
0.86426	0.11027	0.01069	0.01097	0.00382	1	1541.7	23	0.08348	0.02973	998	0.0298	21	0.78	0.07802	787.75	0.099	52.2666	0.3235

## 6. CEA2 Equilibrium Script [Linteris]

```
# This script generates constant volume input files, executes CEA2 equilibrium, and provides
final temperature and pressure as the output.
# Equivalence ratio is determined first from just the fuel and air components. Then a given
percentage of agent is added to the oxidizer to complete the mixture. Mixtures with a relative
humidity of 1 have a water volume fraction on 0.025.
# to run: ./runaucase conc.inp
# This is a script to create the input files to run the NASA CEA2 equilibrium code
# In this example, conc.inp is a vector describing the amount of agent added to a mixture,
typically ranging from 0 to 12%.
# The output is the constant volume equilibrium temperature and pressure for each input mixture.

echo "doing"
pwd

rm jresult.txt

awk 'BEGIN {
mProp=1.00;
AFstoic=15.6808;
#phi must be manually changed
phi=1.00;
AF=AFstoic/phi
MWProp = 44.1;
MWair=29;
MWO2=32;
MWN2=28;

#Agent properties for R123
MWagent = 152.93;
mOxid=(AF)*(MWProp / MWair)*(1 / 4.76)
IdealmolperL = 0.040876319
mtotal=mProp + mOxid
nPieces=10
tempcomma="\", \""
tempspace="\" \""
temp0="$0"
temp1="$1"
temp2="$2"
temp3="$3"
} ;

#-----
# this part creates the input file parts dependent upon the reactants and the run type for CEA2
```

```
#This line builds the input file based on the specified agent and value of phi.
{printf("cat << EOF > j%d.inp\nprob case=nullcase uv\nrho(kg/m**3)=%f\nreac\nname
C3H8 t,k= 298.15 moles= %f\nname CHCL2-CF3 C 2 H 1 CL 2 F 3 moles=
%f\n h,j/mol -757450\nname O2 t,k= 298.15 moles= %f\nname
N2 t,k= 298.15 moles= %f\noutput siunits trace=1.e-9 plot=p t\nend\nEOF\n\n",
FNR+10, ( ( ( mProp / mtotal ) * MWProp ) + ( ( mOxid * (1 - $1 ) ) / mtotal ) * MWair ) + (
( ( mOxid * $1 ) / mtotal ) * MWagent ) ) * IdealmolperL ), mProp, mOxid * $1 * 4.76,
mOxid*(1-$1), mOxid*(1-$1)*3.76)} ;
```

```
#This line prints the command to execute the CEA2 equilibrium program after each input section
{printf("/exports/burner/linteris/NASA.equil.codes/CeaNew/cea2go j%d \n\n", FNR+10)}
'$1 > make+run_inputfiles ;
```

```
#This section groups the inputs together into make+run_inputfiles and then exexutes the file.
echo running make+run_inputfiles
chmod +x make+run_inputfiles
./make+run_inputfiles
```

```
#This line collects the final temperature and pressure outputs which were specified to appear in
the j*.plt output files.
awk '{print}' j???.plt | sed 's/^[ ]*//g;s/[ ]*$//;s/ //g' | awk '{print($1, $2)}' | sed 's/ //g' > jtemp.txt
```

```
#-----
```

## References

1. Bryk, Dale S. "The Montreal Protocol and Recent Developments to Protect the Ozone Layer." *Harvard Environmental Law Review* 15 (1991): 275-98.
2. Calm, James M., Donald J. Wuebbles, and Atul K. Jain. "Impacts on Global Ozone and Climate from Use and Emission of 2,2-Dichloro-1,1,1-Trifluoroethane (HCFC-123)." *Climate Change* 42.2 (1999): 439-74
3. Debora, MacKenzie. "Cheaper Alternatives to CFCs." *Journal of the Mine Ventilation Society of South Africa* 44.1 (1991): 13-15.
4. United States. Environmental Protection Agency. "Revised Guidance Notes for Ozone Depleting Substances, Halon Phase-Out." 2008.
5. Linteris, Gregory T., Donald R. Burgess, Fumiaki Takahashi, Viswanath R. Katta, Harsha K. Chelliah, and Oliver Meier. "Stirred Reactor Calculations to Understand Unwanted Combustion Enhancement by Potential Halon Replacements." *Combustion and Flame* 159 (2012): 1016-025. Web.
6. Hughers Associates, Inc.. ICF Consulting. "Review of the Transition Away From Halons in U.S. Civil Aviation Applications." 2004.
7. Reinhardt, John W. "Behavior of Bromotrifluoropropene and Pentafluoroethane When Subjected to a Simulated Aerosol Can Explosion." Washington, D.C.: Federal Aviation Administration; 2004.
8. Reinhardt, John W. "The Evaluation of Water Mist with and without Nitrogen as an Aircraft Cargo Compartment Fire Suppression System." Washington, D.C.: Federal Aviation Administration; 2002.
9. UNEP: 1993, Handbook for the Montreal Protocol on Substances that Deplete the Ozone Layer (third edition), Ozone Secretariat, Nairobi, Kenya
10. Forster, P., V. Ramaswamy, P. Artaxo, T. Berntsen, R. Betts, D.W. Fahey, J. Haywood, J. Lean, D.C. Lowe, G. Myhre, J. Nganga, R. Prinn, G. Raga, M. Schulz and R. Van Dorland, 2007: Changes in Atmospheric Constituents and in Radiative Forcing. In: *Climate Change 2007: The Physical Science Basis. Contribution of Working Group I to the Fourth Assessment Report of the Intergovernmental Panel on Climate Change* [Solomon, S., D. Qin, M. Manning, Z. Chen, M. Marquis, K.B. Averyt, M.Tignor and H.L. Miller (eds.)]. Cambridge University Press, Cambridge, United Kingdom and New York, NY, USA.
11. Daniel, J.S.; Velders, G.J.M.; A.R. Douglass, P.M.F. Forster, D.A. Hauglustaine, I.S.A. Isaksen, L.J.M. Kuijpers, A. McCulloch, T.J. Wallington, P. Ashford, S.A. Montzka, P.A. Newman, D.W. Waugh, (February 2007). "Halocarbon Scenarios, Ozone Depletion Potentials, and Global Warming Potentials". *Scientific Assessment of Ozone Depletion: 2006*.



World Meteorological Organization, 7bis, avenue de la Paix, Case postale No. 2300, CH-1211 Geneva 2, Switzerland.

12. Wuebbles, Donald J., and Kenneth O. Patten. "Three-Dimensional Modeling of HCFC-123 in the Atmosphere: Assessing Its Potential Environmental Impacts and Rationale for Continued Use." *Environmental Science Technology* 43 (2009): 3208-213.
13. Blake, D., T. Marker, R. Hill, J. Reinhardt, C. Sarkos. "Cargo Compartment Fire Protection in Large Commercial Transport Aircraft." Washington, D.C.: Federal Aviation Administration; 1998.
14. Velders, Guus J.M, A. R. Ravishankara, Melanie K. Miller, Mario J. Molina, Joseph Alcamo, John S. Daniel, David W. Fahey, Stephen A. Montzka, and Stefan Reimann. "Preserving the Montreal Protocol Climate Benefits by Limiting HFCs." *Science* 335 (2012): 922-23.
15. Velders, Guss J.M, Stephan O. Anderson, John S. Daniel, David W. Fahey, and Mack McFarland. "The Importance of the Montreal Protocol in Protecting Climate." *PNAS* 104.12 (2007): 4814-819.
16. Tokarsky E.W, Robin M.L. Clean fire extinguishments for DoD applications. *AMMTIAC Quarterly* 2011, 6(1):11-14.
17. Metghalchi, M., and J. C. Keck. "Laminar Burning Velocity of Propane-Air Mixtures at High Temperature and Pressure." *Combustion and Flame* 38 (1980): 143-54.
18. Takizawa, Kenji, Akifumi Takahashi, Kazuaki Tokuhashi, Shigeo Kondo, and Akira Sekiya. "Burning Velocity Measurements of Fluorinated Compounds by the Spherical-Vessel Method." *Combustion and Flame* 141 (2005): 298-307.
19. Williams, F. A. *Combustion Theory*. N.p.: Addison Wesley, 1985.
20. G.T. Linteris, J. A. Manion, D.R. Burgess. "Understanding Unwanted Combustion Enhancement by Potential Halon Replacements". NIST Publication. 2010 Annual Report for the Boeing Company; 2010.
21. Gordon, S, McBride, BJ. Computer program for calculation of complex chemical equilibrium compositions and applications. NASA Reference Publication 1311, Cleveland, OH: NASA Glenn Research Center; 1996.
22. Shebeko, Yu N., V. V. Azatyan, I. A. Bolodian, V. Yu Navzenya, S. N. Kopylov, D. Yu Shebeko, and E. D. Zamishevski. "The Influence of Fluorinated Hydrocarbons on the Combustion of Gaseous Mixtures in a Closed Vessel." *Combustion and Flame* 121 (2000): 542-47.
23. Turns, Stephen R. *An Introduction to Combustion: Concepts and Applications*. Boston: WCB/McGraw-Hill, 2000.

24. P. Glarborg, R.J. Kee, J.F. Grcar, J.A. Miller, PSR: A FORTRAN Program for Modeling Well-Stirred Reactors, SAND86-8209, Sandia National Laboratories, 1986.
25. Sheen, DA, You, XQ, Wang, H, Lovas, T. Spectral uncertainty quantification, propagation and optimization of a detailed kinetic model for ethylene combustion. Proceedings of the Combustion Institute 2009; 32:535-542.
26. Wang, H, You, X, Jucks, KW, Davis, SG, Laskin, A, Egolfopoulos, F, Law, CK. USC Mech Version II. High-temperature combustion reaction model of H<sub>2</sub>/CO/C<sub>1</sub>-C<sub>4</sub> compounds. [http://ignis.usc.edu/USC\\_Mech\\_II.htm](http://ignis.usc.edu/USC_Mech_II.htm), Los Angeles, CA: University of Southern California; 2007.
27. Li, J, Kazakov, A, Chaos, M, Dryer, FL, "Chemical Kinetics of Ethanol Oxidation", In: Fifth Joint Meeting of the U.S. Sections of The Combustion Institute, Proceedings of the Fifth Joint Meeting of the U S Sections of The Combustion Institute, Combustion Institute, Pittsburgh, PA, (2007).
28. Li, J, Kazakov, A, Dryer, FL. Ethanol pyrolysis experiments in a variable pressure flow reactor. International Journal of Chemical Kinetics 2001; 33:859-867.
29. Li, J, Kazakov, A, Dryer, FL. Experimental and numerical studies of ethanol decomposition reactions. Journal of Physical Chemistry A 2004; 108:7671-7680.
30. Burgess, DR, Zachariah, MR, Tsang, W, Westmoreland, PR. Thermochemical and chemical kinetic data for fluorinated hydrocarbons. Progress in Energy and Combustion Science 1995; 21:453-529.
31. Burgess, D, Zachariah, MR, Tsang, W, Westmoreland, PR. Thermochemical and chemical kinetic data for fluorinated hydrocarbons. NIST Technical Note 1412, Gaithersburg, MD: National Institute of Standards and Technology; 1995.
32. Babushok, V, Noto, T, Burgess, DRF, Hamins, A, Tsang, W. Influence of CF<sub>3</sub>I, CF<sub>3</sub>Br, and CF<sub>3</sub>H on the high-temperature combustion of methane. Combust Flame 1996; 107:351-367.
33. Babushok, VI, Burgess, DRF, Tsang, W, Miziolek, AW. Simulation studies on the effects of flame retardants on combustion processes in a plug reactor. In: Halon Replacements. 1995. 275-288.
34. Leylegian JC, Law CK, Wang H: "Laminar flame speeds and oxidation kinetics of tetrachloromethane"; 1998.
35. Leylegian JC, Zhu DL, Law CK, Wang H: "Experiments and numerical simulation on the laminar flame speeds of dichloromethane and trichloromethane". Combustion and Flame 1998, 114(3-4):285-293.

36. Babushok V.I., Linteris G.T., Meyer O.C., Pagliaro J.L.: "Flame Inhibition by CF<sub>3</sub>CHCl<sub>2</sub> (HCFC-123)." Submitted to Combustion and Flame. 2012
37. Linteris, G.T., Takahashi F., Katta V., Chelliah H., Meier O.: "Thermodynamic Analysis of Suppressant-Enhanced Overpressure in the FAA Aerosol Can Simulator." Proceedings of the Tenth International Symposium, International Association for Fire Safety Science. 2011.
38. Takizawa, Kenji, and Kazuaki Tokuhashi. "Flammability Assessment of CH<sub>2</sub>=CFCl<sub>2</sub>: Comparison with Fluoralkenes and Fluoroalkanes." *Journal of Hazardous Materials* 172 (2009): 1329-338.
39. Gmurchyk, G. W., Grosshandler, W. L., Lowe, D. L., *Proceedings of the 4<sup>th</sup> International Symposium on Fire Safety Science*, Ottawa, Canada, 1995, p. 925.